REPORT DOCUMENTATION PAGE

1a. REPORT SECURITY CLASSIFICATION	1b. RESTRICTIVE MARKINGS
Unclassified	

2a. SECURITY CLASSIFICATION AUTHORITY

3. DISTRIBUTION / AVAILABILITY OF REPORT

Approved for public release;
distribution unlimited.

AD-A224 981

5. MONITORING ORGANIZATION REPORT NUMBER(S)

ARO 22583.15-LS

6a. NAME OF PERFORMING ORGANIZATION	6b. OFFICE SYMBOL (If applicable)	7a. NAME OF MONITORING ORGANIZATION
Harvey Alan Berman. School of Pharmacy		U. S. Army Research Office

6c. ADDRESS (City, State, and ZIP Code)	7b. ADDRESS (City, State, and ZIP Code)
335 Hochstetter Hall, Biochemical Pharmacol. State University of New York at Buffalo Buffalo, New York 14260	P. O. Box 12211 Research Triangle Park, NC 27709-2211

8a. NAME OF FUNDING / SPONSORING ORGANIZATION	8b. OFFICE SYMBOL (If applicable)	9. PROCUREMENT INSTRUMENT IDENTIFICATION NUMBER
U. S. Army Research Office		DAAG29-85-K-0083

8c. ADDRESS (City, State, and ZIP Code)	10. SOURCE OF FUNDING NUMBERS			
P. O. Box 12211 Research Triangle Park, NC 27709-2211	PROGRAM ELEMENT NO.	PROJECT NO.	TASK NO.	WORK UNIT ACCESSION NO.

11. TITLE (Include Security Classification)

Acetylcholinesterase Chirality and Cellular Mechanisms
of Organophosphonate Toxicity

12. PERSONAL AUTHOR(S)

Berman, Harvey A.

13a. TYPE OF REPORT	13b. TIME COVERED	14. DATE OF REPORT (Year, Month, Day)	15. PAGE COUNT
Final	FROM 6/1/85 TO 3/31/90	1990-6-11	

16. SUPPLEMENTARY NOTATION

The view, opinions and/or findings contained in this report are those
of the author(s) and should not be construed as an official Department of the Army position,
policy, or decision, unless so designated by other documentation.

17.	COSATI CODES		18. SUBJECT TERMS (Continue on reverse if necessary and identify by block number)
FIELD	GROUP	SUB-GROUP	Acetylcholinesterase; organophosphates; organophosphonates; chirality; cellular toxicity.

19. ABSTRACT (Continue on reverse if necessary and identify by block number)

These studies concern the chiral reactivity of AchE, and examine the topography of the enzyme subunit. Several independent kinetic and equilibrium indices of ligand orientation are employed: bimolecular inhibition, oxime reactivation, aging, and equilibrium dissociation constants. Organic synthesis is an integral part of these studies and we developed several families of achiral and chiral, and fluorescent and non-fluorescent organophosphonates and reversible noncovalent fluorescent probes. These agents are employed in study of AchE from *Torpedo*, as one means for probing subunit topography, as well as in *in vivo* and *in vitro* studies concerning cellular regulation of AchE.

20. DISTRIBUTION / AVAILABILITY OF ABSTRACT	21. ABSTRACT SECURITY CLASSIFICATION
☐ UNCLASSIFIED/UNLIMITED ☐ SAME AS RPT. ☐ DTIC USERS	Unclassified

22a. NAME OF RESPONSIBLE INDIVIDUAL	22b. TELEPHONE (Include Area Code)	22c. OFFICE SYMBOL

DD FORM 1473, 84 MAR
83 APR edition may be used until exhausted.
All other editions are obsolete.

STATEMENT OF PROBLEM STUDIED

This contract concerned chiral reactivity of AchE, and examined the topography of the enzyme subunit with respect to a number of independent kinetic and equilibrium indices of ligand orientation: bimolecular inhibition, oxime reactivation, aging, and equilibrium dissociation constants. Organic synthesis was an integral part of these studies and we developed several families of achiral and chiral, and fluorescent and non-fluorescent organophosphonates and reversible noncovalent probes. These agents were employed in study of AchE from *Torpedo,* as one means for probing subunit topography, as well as in *in vivo* and *in vitro* studies concerning cellular regulation of AchE.

Since all studies are either published or *in press* and have been described in previous semi-annual Progress Reports, this *FINAL REPORT* will highlight our salient findings and will reference the appropriate papers (enclosed). Copies of those papers that have been submitted but are currently under peer review (*15,16*) and those that are *in press* (*12-14*) are not yet available so are not enclosed.

SUMMMARY OF RESEARCH FINDINGS

<u>Fluoresent probes of acetylcholinesterase</u>. We have developed fluorescent methylphosphonates (NBD-aminoalkyl methylphosphonofluoridates) that irreversibly modify the active center serine (2); these agents found utility in our physiological studies on the ...ntral medulla oblongata (*1,4*). Also, since they are environmentally sensitive, we are currently employing ther; s advantageous use in our examination of electrostatic relationships at the surface of acetylcholinesterase (AchE) from *Torpedo* and butyrylcholinesterase (BuchE) from human plasma (*15*). In addition we have developed reversible fluorescent agents, hexidium and decidium, that probe sites remote from the active center (*5,6,8*). The latter agents have found utility in examining aging of organophosphonyl conjugates of AchE and, in particular, in providing an assay independent of enzyme activity for monitoring aging-unduced loss of the alkyl group (*6, 11*).

<u>Inhibition, reactivation and aging of organophosphonyl conjugates of AchE</u>. Our studies concern inhibition, reactivation, and aging of organophosphonyl conjugates of AchE (*5,6,10,11*). We have found that while aging of these conjugates shows a strong dependence on ionic strength and pH of the medium, the reaction kinetics are not consistent with participation of a specific amino acid residue in this process. As such, these studies indicated that the bulk properties of the enzyme active center, rather than a defined amino acid residue, promote aging. Hence, the aging mechanism provides an index of the thermodynamic activity of water within the active center.

As a means for extending these studies, we developed an experimentally feasible series of reactions for synthesis of homologous enantiomeric organophosphorus agents in which assignment of configuration was unambiguous (*10*). A number of enantiomeric agents were synthesized; a wide range of inhibition constants was observed. Bimolecular inhibition constants spanned 10^2-10^9 M^{-1}-min^{-1}, equilibrium dissociation constants 10^{-3}-10^{-7} M, and phosphonylation constants less than 1 to greater than 300 min^{-1}. A general but not absolute preference for the S_P-enantiomer was observed. Cases were observed in which there was either no chiral preference or an inversion in chiral preference. These results illustrate clearly that *there exists no absolute chiral preference of AchE for methylphosphonates*, and that any observed stereospecificty is more critically dependent on the nature of the ester moiety (-OR) and leaving group (-SR') surrounding phosphorus than on the absolute configuration about the tetrahedral phosphorus. These studies represent the first unequivocal demonstration that *R_P-enantiomeric conjugates formed from bulky branched alkyl methylphosphonates undergo neither oxime reactivation nor aging.*

The "Wilsonian" model of the enzyme active center, derived by I. B. Wilson from study of planar synthetic substrates, indicated the presence of an anionic site within 5A of the nucleophilic serine. As evidenced by chiral criteria, however, our studies indicate that the active center contains two topographically distinct sites within a

circumscribed distance from the nucleophilic serine. In addition to the anionic site, there exists within 5A of the reactive serine a hydrophobic *alkyl-binding region* in close proximity of the active center serine. This region is of importance since, as deduced from the reaction kinetics, association of alkyl groups within this region accelerates bimolecular reaction.

Probing the acyl region of AchE with alkylphosphonates. In light of these studies, irreversible inhibition of the enzyme active center serine can occur through occupation of either the anionic site or the hydrophobic site. As a demonstration of these added degrees of freedom in inhibition, we examined reaction of AchE with alkylphosphonofluoridates containing *n*-alkyl chains spanning C_1-C_6 alkyl groups. All alkylphosphonofluoridates were highly reactive ($k_i > 10^6$ M^{-1}-min^{-1}) leading to the conclusion that, while AchE expresses a chiral preference for S_p-over R_p-enantiomers, the final orientation achieved by the organophosphonate on the enzyme surface is contingent on which one of the four tetrahedral faces undergo attach by the reactive serine. The identity of this tetrahedral face will be governed, in turn, by the non-covalent interactions between the different groups surrounding phosphorus and the enzyme surface. These studies are currently in progress under ARO PROPOSAL NUMBER: 26582-LS; CONTRACT NUMBER: DAAL03-89-K-0063.

Cellular regulation of AchE. Finally, our studies concern cellular regulation of AchE and were undertaken as one means for understanding the chronic effects of organophosphonates on cell metabolism. During these studies we observed that calcium-entry blockers such as the dihydropyridine nifedipine caused marked reductions in the amounts of AchE molecular forms in primary tissue cultures of avian pectoral muscle (13). These reductions were time-dependent, requiring passage of 3 hours prior to any observable response, dose-dependent, with principal actions occurring in the 1-100 nM range, greater on the 7S and 19S forms than on the 11.4S form, and occurred almost exclusively with *intra*cellular AchE coincident with a 2-fold reduction in the rate of secretion. The effects were markedly more pronounced in skeletal muscle than in neurons, and differed from those observed for verapamil, diltiazem, and the calcium ionophore A23187. These reductions indicate that nifedipine causes a reduction in AchE biosynthesis. Since AchE forms are thought to arise from a single gene, these findings imply a linkage in skeletal muscle between transcription and post-transcriptional processing of mRNA and ligand occupation of the dihydropyridine receptor. This finding is novel and represents the first demonstration of a cell surface receptor mediated event that leads to an alteration in cholinergic biosynthesis. In a related series of studies we have found that denervation of *anterior tibialis* in rat leads to alterations in the non-denervated muscle in the contralateral limb and in non-denervated diaphragm (7,12). These studies indicated the existence of a soluble diffusible neurotrophic factor that alters intraellular metabolism of AchE.

PUBLICATIONS

1. Edery, H. and Berman, H.A. "Yohimbine antagonism of the vasodepression elicited by organophosphates applied on ventral medulla oblongata". J. Autonom, Nerv. Syst., 14, 229-238 (1985).
2. Berman, H.A., Olshefski, D.F., Gilbert, M., and Decker, M.M. "Fluorescent phosphonate labels for serine hydrolases: kinetic and spectroscopic properties of (7-nitrobenz-2-oxa-1,3-diazole)aminoalkyl methylphosphonofluoridates and their conjugates with acetylcholinesterase molecular forms". J. Biological Chemistry, 260, 3462-3468 (1985).
3. Berman, H.A., Yguerabide, J. and Taylor, P. "Flexibility of the molecular forms of acetylcholinesterase measured with steady-state and nanosecond fluorescence polarization spectroscopy". Biochemistry, 24, 7140-7147 (1985).
4. Edery, H., Geyer, M.A., Taylor, P. and Berman*, H.A. "Target sites for anticholinesterases on the ventral surface of the medulla oblongata: Hypotension elicited by organophosphorus agents." J. Autonomic Pharmacology, 6, 195-206 (1986).
5. Berman, H.A. and Decker, M.M. "Kinetic, equilibrium, and spectroscopic studies on cation association at the active center of acetylcholinesterase: Topographic distinction between trimethyl and trimethylammonium sites". Biochim. Biophys. Acta, 872, 126-133 (1986).

6. Berman, H.A. and Decker, M.M. "Kinetic, equilibrium and spectroscopic studies on dealkylation ("Aging") of alkyl organophosphonyl-acetylcholinesterase: Electrostatic control of enzyme topography". **J. Biological Chemistry, 261,** 10646-10652 (1986).

7. Berman, H.A., Decker, M.M. and Jo, S. "Reciprocal regulation of acetylcholinesterase and butyryl-cholinesterase in mammalian skeletal muscle", **Developmental Biology, 120,** 154-161 (1987).

8. Berman, H.A., Decker, M.M., Nowak, M.W., Leonard, K.J., McCauley, M., Baker, W.M., and Taylor, P. "Site selectivity of fluorescent bisquaternary phenanthridinium ligands for acetylcholinesterase". **Molecular Pharmacology, 31,** 610-616 (1987).

9. Johnson, D. A., Brown, R. D., Herz, J. M., Berman, H. A., Andreasen, G. L. and Taylor, P. "Decidium: A novel fluorescent probe of the agonist/antagonist and noncompetitive inhibitor sites on the nicotinic acetylcholine receptor". **J. Biological Chemistry, 262,** 14022-14029 (1987).

10. Berman, H.A. and Leonard, K.J. "Chiral reactions of acetylcholinesterase probed with enantiomeric methylphosphonothioates: Noncovalent determinants of enzyme chiral preference", **J. Biological Chemistry, 264,** 3942-3950 (1989).

11. Berman, H.A. and Decker, M.M. "Chiral nature of covalent methylphosphonyl conjugates of acetyl-cholinesterase", **J. Biological Chemistry, 264,** 3951-3956 (1989).

12. Decker, M.M. and Berman, H.A. (1990) "Denervation-induced alterations in acetylcholinesterase in denervated and non-denervated muscle" **Exp. Neurol., 109** (in press; not enclosed).

13. Decker, M.M. and Berman, H.A. (1990) "Dihydropyridine receptor regulation of acetylcholinesterase in avian skeletal muscle." **J. Biol. Chem., 265** (in press; not enclosed).

14. Berman, H.A., Leonard, K.J., and Nowak, M.W. (1990) "Function of the peripheral anionic site of acetyl-cholinesterase" IN Proceedings of the Third International Meeting on Cholinesterase (in press; not enclosed).

15. Berman, H.A. and Leonard, K.J. (1990) "Ligand exclusion on acetylcholinesterase: Role of the peripheral anionic site." **Biochemistry** (submitted 5/90; not enclosed).

16. Jo, S. and Berman, H.A. (1990) "Influence of parasympathetic and sympathetic denervation on cholinergic in chick heart." **J. Neurochem.** (submitted, 6/90; not enclosed).

PERSONNEL

      a. Mildred M. Decker, Senior laboratory technician.
      b. Kathryn J. Leonard, Laboratory technician.
      c. Michael Rusiniak, Graduate student.
      d. Sangmee Jo, Graduate student.
      e. Mark W. Nowak, Graduate student.
      f. Bruce M. Bechle, Lab technician
      g. David Luo, Graduate student

DEGREES AWARDED

Mildred M. Decker, MSc. (May, 1989) "Regulation of skeletal muscle acetylcholinesterase biosynthesis by nerve and calcium".

Sangmee Ahn Jo, PhD (February, 1990) "Influence of innervation on protein metabolism in avian heart".

Decidium

A NOVEL FLUORESCENT PROBE OF THE AGONIST/ANTAGONIST AND NONCOMPETITIVE INHIBITOR SITES ON THE NICOTINIC ACETYLCHOLINE RECEPTOR[*]

David A. Johnson‡, R. Dale Brown§, Jeffrey M. Herz§, Harvey Alan Berman¶, Grai L. Andreasen§, and Palmer Taylor§

From the ‡Division of Biomedical Sciences, University of California, Riverside, California 92521, the §Department of Pharmacology, University of California, San Diego, La Jolla, California 92093, and the ¶Department of Biochemical Pharmacology, State University of New York at Buffalo, Buffalo, New York 14260

We have examined the interaction of the nicotinic acetylcholine receptor with decidium diiodide, a bisquaternary analogue of ethidium containing 10 methylene groups between the endocyclic and trimethylamino quaternary nitrogens. Decidium inhibits mono-$[^{125}I]$iodo-α-toxin binding, inhibits agonist-elicited $^{22}Na^+$ influx in intact cells, augments agonist competition with mono-$[^{125}I]$iodo-α-toxin binding, and enhances $[^3H]$phencyclidine (PCP) binding to a noncompetitive inhibitor site. These effects occur over similar concentration ranges (half-maximum effects between 0.1 and 0.4 μM). Thus, decidium binds to the agonist site and converts the receptor to a desensitized state exhibiting increased affinity for agonist and heterotropic inhibitors. These properties are similar to metaphilic antagonists characterized in classical pharmacology. At higher concentrations decidium associates directly with the noncompetitive inhibitor site identified by $[^3H]$phencyclidine binding. Dissociation constants of decidium at this site in the resting and desensitized states are determined to be 29 and 1.2 μM, respectively. Analysis of fluorescence excitation and emission maxima reveal that binding to both the agonist and noncompetitive inhibitor sites is associated with ~2-fold enhancement of fluorescence. The excitation maximum for decidium bound at the agonist site appears at 490 nm while that for decidium bound at the noncompetitive inhibitor site appears at 530 compared to 480 nm in buffer. These results suggest that decidium experiences a more hydrophobic environment upon binding to the nicotinic acetylcholine receptor sites, particularly to the noncompetitive inhibitor site. Fluorescence energy transfer between N'-fluorescein isothiocyanate-lysine-23 α-toxin (FITC-toxin), and decidium is not detected when each is bound to one of the two agonist sites on the receptor. This allows a minimal distance to be estimated between fluorophores. In contrast, energy transfer is observed between decidium nonspecifically associated with the membrane or with nonspecific sites and the FITC-toxin at the agonist sites.

The nicotinic acetylcholine receptor (AcChR)[1] represents a prototypic transmembrane ligand-regulated ion channel. Coupling of receptor occupation with ion permeability arises from an interplay between interconvertible functional states, modulated by the history of exposure to agonist or a variety of heterotropic ligands, such as phencyclidine (PCP) and local anesthetics. The emerging description of ligand-response coupling reveals a dynamic receptor entity possessing discrete but allosterically interactive sites and functional domains on the receptor oligomer.

Fluorescent ligands containing 5-dimethylaminonaphthalene-1-sulfyl (Dansyl) (Heidmann and Changeux, 1979), pyrenebutyl (Tan and Barrantes, 1980), or 7-nitrobenzo-2-oxa-1,3-diazole (Prinz and Maelicke, 1983a, 1983b; Bolger et al., 1984) moieties have been employed to characterize effector sites and mechanisms underlying functional transitions of the nicotinic receptor. These ligands emit at wavelengths shorter than 550 nm. A ligand which emits at wavelengths greater than 600 nm would be useful for assessing intersite distances through excitation energy transfer. To this end, we have characterized the interaction of decidium diiodide with the AcChR. Decidium is a fluorescent phenylphenanthridium analogue of ethidium which contains 10 methylene groups between the endocyclic quaternary nitrogen and the exocyclic trimethylamino quaternary nitrogen. Hence, it contains an interquaternary distance identical to decamethonium and its congeners which have been widely studied in nicotinic receptor function.
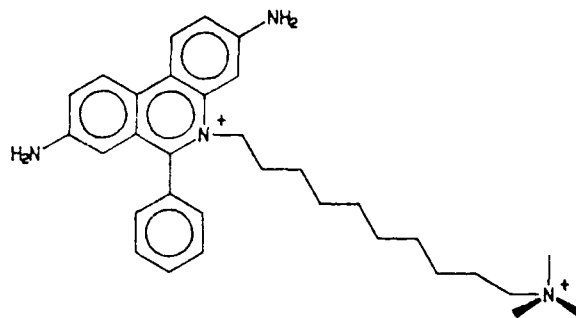
STRUCTURE 1

In the present study we describe the pharmacological, biochemical, and spectroscopic properties of decidium upon interaction with the AcChR. Dipolar energy transfer is em-

[1] The abbreviations used are: AcChR, nicotinic acetylcholine receptor; FITC-toxin, N'-fluorescein isothiocyanate-lysine-23 cobra α-toxin; α-toxin, Naja naja siamensis 3 α-toxin; ^{125}I-labeled α-toxin, α-mono-$[^{125}I]$iodo-α-toxin; PCP, phencyclidine; K_p, protection constant.

ployed to determine the distance between the two AcChR agonist-binding sites using N'-fluorescein isothiocyanate-lysine-23 cobra α-toxin (FITC-toxin) bound to one and decidium to the other.

To characterize the properties of decidium, we utilized both the BC3H-1 clonal muscle cell line and AcChR-enriched membrane fragments from *Torpedo californica*. BC3H-1 cells grow in monolayer cultures and elaborate uniformly distributed surface AcChRs permitting simultaneous measurement of receptor occupation and functional response in the same population of intact cells. *Torpedo* electric organs provide highly enriched source of receptors for fluorescence measurements.

EXPERIMENTAL PROCEDURES

Materials—Cell culture media and fetal calf serum were obtained from GIBCO. Radionuclides, ^{125}I and ^{22}Na$^+$, and [^{3}H]PCP were obtained carrier-free from Du Pont-New England Nuclear. PCP was obtained from the National Institute of Drug Abuse. d-Tubocurarine chloride was a gift from Lilly. Dinaphthyldecamethonium was a gift from Dr. H. P. Rang (University College, London, England). Proadifen was obtained from Smith Kline, and French. Meproadifen was prepared by methylating proadifen with iodomethane. Lidocaine and carbamylcholine were from Sigma. The synthesis and chemical characterization of decidium is described in Berman *et al.* (1987). Freshly prepared solutions of decidium in buffer were clarified by filtration and the decidium concentration determined from the absorbance at 480 nm (ϵ_{480} = 6000 M^{-1} cm^{-1}). Concentrated stock solutions were dissolved in acetonitrile, protected from light, and stored at −10 °C. FITC-toxin was prepared as described elsewhere (Johnson and Taylor, 1982) and purified by column isoelectric focusing (Weiland *et al.*, 1976). Cobra α-toxin (*siamensis 3*) was isolated following the method of Karlsson *et al.* (1971) from *Naja naja siamensis* venom (Miami Serpentarium, Salt Lake City, UT). Mono-[^{125}I]iodo-α-toxin (*siamensis 3*) (^{125}I-labeled α-toxin) was prepared and separated from noniodinated and diiodo species by column isoelectric focusing. All other reagents were at least reagent grade. Except where noted, all binding and spectroscopic analyses were performed with samples suspended in 100 mM NaCl, 10 mM sodium phosphate buffer at pH 7.4.

Receptor Isolation—Receptor-rich membrane fragments were isolated from *T. californica* electric organ following published procedures (Johnson and Yguerabide, 1985; Reed *et al.*, 1975). The specific binding activities of the receptor preparations were measured by adsorption of ^{125}I-labeled α-toxin-receptor complexes onto DEAE-cellulose filters (Schmidt and Raftery, 1975) and ranged between 1 and 2 nmol of α-toxin-binding sites/mg of protein.

Assays of Receptor Occupation and Agonist-stimulated Permeability Response—Kinetic assays to measure ligand competition with the initial rate of ^{125}I-labeled α-toxin binding to AcChR in *Torpedo* membranes were performed using Whatman DE81 filter discs to adsorb selectively the receptor-toxin complex as described previously (Weiland *et al.*, 1976). To reduce nonspecific adsorption of ^{125}I-labeled α-toxin, the filter discs were acid-washed as follows. Filters were placed in a 43 °C HCl/methanol solution (1:2, v/v) and allowed to cool to room temperature over a 45-min period. The filters were washed three times in distilled water with an overnight soak and then dried before use.

Assays of ligand competition with initial rates of ^{125}I-labeled α-toxin binding and agonist stimulated ^{22}Na$^+$ permeability in intact BC3H-1 cells were performed as described previously (Sine and Taylor, 1980; Brown and Taylor, 1983).

[^{3}H]PCP Binding—Equilibrium binding of radiolabeled PCP was measured by a modification of the centrifugation assay of Heidmann *et al.* (1983)as described by Palma *et al.* (1986). Competition binding experiments were analyzed by the LIGAND nonlinear curve-fitting program developed by Munson and Rodbard (1980). PCP affinity toward the desensitized and resting states were determined to be 0.4 and 2.0 μM, respectively. Data points are the mean of duplicate samples.

Steady-state Spectroscopy—Steady-state fluorescence and absorption measurements were made with a SPEX F111A spectrofluorometer and a Perkin-Elmer Lambda 3B spectrophotometer, respectively.

Fluorescence Titrations of Decidium Association with the Receptor—Titrations were carried out in 1-cm cuvettes using a water-

jacketted, four-sample turetted compartment. All fluorescence values were corrected for dilution resulting from added titrant, incident light scatter, and innerfilter effects. Except where noted, excitation and emission wavelengths were 290 and 620 nm, respectively. In the case of direct titrations with decidium, fluorescence contributions of the free ligand were subtracted from total fluorescence, and the specific fluorescence enhancement *versus* ligand concentration was plotted directly.

For measurements of competition with other ligands, decidium and receptor concentrations were 2.5 and 0.25 μM, respectively. Data are plotted to the formulation

$$\log\left[\frac{f_h - f}{f - f_c}\right] = n_H\log\frac{K_D}{K_C} + n_H\log\frac{[C]}{[D]} \tag{1}$$

where f, f_h, and f_c are the observed decidium fluorescence, fluorescence when sites on the receptor are fully occupied, and the fluorescence when decidium is fully dissociated from the receptor. [D] and [C] represent the estimated free decidium and competing ligand concentrations, and K_D and K_C represent their respective dissociation constants (Taylor and Lappi, 1975). Equation 1 assumes that $[D] \gg K_D$ and that [D] is in excess of its binding sites.

Fluorescence Lifetime Analysis—Fluorescence lifetimes were determined by the single-photon-counting technique using an EEY Scientific nanosecond fluorescence spectrofluorometer (La Jolla, CA) equipped with a high pressure hydrogen arc lamp. Excitation and emission bands of the FITC-toxin were selectively monitored with Oriel 450 nm broad and 560 nm narrow band interference filters, respectively. The filters used for measurement of the FITC-toxin lifetime were selected to eliminate interference from decidium emission. In addition to the chromatic filters, Polaroid HNP'B dichroic film polarizers (Norwood, MA) were placed in the excitation and observation paths. The emission polarizer was rotated at an angle of 55° relative to the vertically oriented excitation polarizer to eliminate anisotropic contributions to the observed decay. Light scatter was corrected by subtracting the decay curves for samples containing all the components except the fluorophore. The instrumental arrangement and principles of data treatment have been discussed in detail (Yguerabide, 1972; Johnson and Yguerabide, 1985).

Energy Transfer—The efficiency of dipolar resonance energy transfer between a discrete donor and acceptor pair is related to the distance (R) separating the pair by Equation 2 (Forster, 1965).

$$R = R_0(1/E - 1)^{1/6} \tag{2}$$

R_0, the distance at which transfer efficiency equals 50%, is 9.765 × 10^3 ($\kappa^2 J Q_D n^{-4})^{1/6}$. The overlap integral, J, between excited state donor and acceptor dipoles is the integrated area of overlap between the donor emission spectrum, $I_D(\lambda)$, and the acceptor absorption spectrum, $\epsilon_A(\lambda)$ (Equation 3).

$$J = \frac{\int I_D(\lambda)\epsilon_A(\lambda)\lambda^4 d\lambda}{\int I_D(\lambda)d\lambda} \tag{3}$$

Q_D denotes the donor quantum yield in the absence of acceptor and n represents the refractive index of the medium between donor and acceptor. κ^2, the orientation factor, accounts for the relative orientation of the donor emission and acceptor absorption transition dipoles. λ is the wavelength in cm.

When donor and acceptor are at separate sites on a macromolecule, the efficiency of energy transfer (E_D) can be measured by

$$E_D = 1 - \tau_{DA}/\tau_D \tag{4}$$

where τ_{DA} and τ_D are the fluorescence lifetimes of the donor in the presence and absence of acceptor, respectively (Forster, 1959).

The distance relationships between FITC-toxin and decidium bound to the agonist sites on the AcChR was examined after 15% of the agonist sites were occupied with the FITC-toxin. This value was chosen as a compromise between maximizing the signal from FITC-toxin while minimizing the number of receptors with both agonist sites occupied with FITC-toxin. Since FITC-toxin binds with equal probability to either of the two agonist sites, the formula for a binomial distribution was used to estimate the proportion of doubly *versus* singly occupied receptors (Damle and Karlin, 1978). With 15% of all the α-toxin-binding sites occupied by FITC-toxin, 82% of the FITC-toxin-occupied receptors will have only one toxin molecule bound, and 17% will have two FITC-toxin molecules bound (cf. Table I in Damle and Karlin, 1978). After the FITC-toxin was incubated
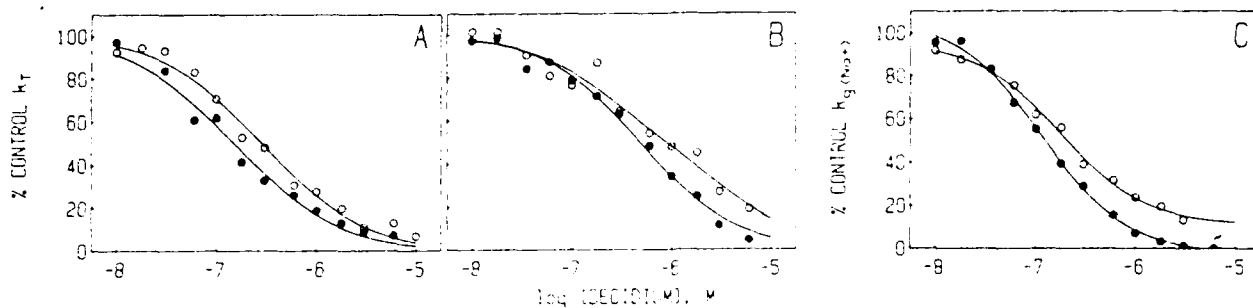
FIG. 1. **Decidium inhibition of initial rates of cobra** ^{125}**I-labeled α-toxin and carbamylcholine-stim-ulated** ^{22}**Na$^+$ influx in** *Torpedo* **membranes and BC3H-1 cells.** Initial rates of ^{125}I-labeled α-toxin binding to AcChR in *Torpedo* membrane fragments (*A*) or monolayer BC3H-1 cultures (*B*) were measured in the presence of the indicated decidium concentrations. Data were normalized to the rate of α-toxin binding in the absence of decidium. *C*, initial rates of carbamylcholine-stimulated ^{22}Na$^+$ influx were measured in BC3H-1 cells in the presence of 60 μM carbamylcholine plus the indicated decidium concentrations. Experimental determinations were made in duplicate. *Filled circles* ($\bullet$), equilibrium exposure (30 min) to buffer containing the indicated decidium concentrations followed by initial rate measurements of either ^{125}I-labeled α-toxin or carbamylcholine-stimulated ^{22}Na$^+$ influx in the presence of the indicated decidium concentrations. *Open circles* (O), after equilibration in buffer alone for 30 min, the instantaneous addition of decidium and α-toxin (*panels A* and *B*) or 60 μM carbamylcholine (*panel C*) starts the respective initial rate measurements. The *solid lines* represent nonlinear best fits to the Hill equation.

with the AcChR, the remaining unoccupied sites were occupied by a near saturating concentration of decidium, 10 μM. PCP (100 μM) was present to prevent decidium binding to the noncompetitive inhibitor site.

RESULTS

Decidium Inhibition of Initial Rate of ^{125}*I-Labeled α-Toxin Binding and Agonist-stimulated* ^{22}*Na$^+$ Permeability*—Decidium inhibition of the initial rate of ^{125}I-labeled α-toxin binding to both *Torpedo* AcChR-enriched membrane fragments and intact BC3H-1 cells was examined after instantaneous and prolonged (30 min) exposure to decidium. Decidium inhibits α-toxin binding to AcChR in *Torpedo* membranes (Fig. 1*A*) and in intact BC3H-1 cells (Fig. 1*B*). In each case the binding profiles exhibit Hill coefficients (n_H) less than unity. Decidium also inhibits ^{22}Na$^+$ influx stimulated by carbamylcholine in BC3H-1 cells (Fig. 1*C*) at slightly lower concentrations but with a somewhat steeper profile (Table I). As seen in *Torpedo* (Neubig and Cohen, 1979; Weiland and Taylor, 1979) and in BC3H-1 cells (Sine and Taylor, 1981), the Hill slope of less than unity for occupation suggests nonequivalence of decidium K_d for the two agonist sites on the receptor. The dependence on lower antagonist concentrations for blockade of the functional response is consistent with the concept that occupation of only one of the two sites is adequate to achieve functional antagonism, as documented for the classical antagonists (Sine and Taylor, 1981). In control experiments, decidium alone did not increase ^{22}Na$^+$

permeability over basal values, indicating that it has no partial agonist activity (data not shown).

The decidium protection constants decreased 2–4-fold when decidium was added 30 min prior to instead of simultaneously with radiolabeled α-toxin addition (Fig. 1, Table I). This observation suggests that decidium possesses a limited capacity to convert AcChR to a state which displays increased affinity for decidium. Such a conversion in AcChR state might occur by decidium acting at the agonist site as a metaphilic antagonist (Rang and Ritter, 1970a, 1970b) or by acting at an allosteric site as a noncompetitive, heterotropic inhibitor. In both cases, a slow conversion to a state possessing a higher affinity for decidium is predicted.

Decidium Inhibition of Agonist Activation of AcChR Permeability Response—To examine the mechanism of decidium inhibition, the concentration dependence for carbamylcholine activation of ^{22}Na$^+$ permeability was measured in BC3H-1 cells in the presence of decidium. For comparison, a metaphilic antagonist, dinaphthyldecamethonium (Rang and Ritter, 1970a, 1970b), and a classical antagonist, *d*-tubocurarine were also examined. Increasing decidium concentrations progressively shift the carbamylcholine concentration-response curve to higher agonist concentrations as well as reduce the maximal response obtained at saturation (Fig. 2*A*). This behavior indicates both competitive and noncompetitive components of decidium inhibition are present. Like decidium, dinaphthyldecamethonium displays apparent noncompetitive inhibition, consistent with conversion of AcChR to a desensitized state incapable of channel opening (Fig. 2*B*). *d*-Tubo-

TABLE I

Protection constants, K_p, for decidium inhibition of initial rates of carbamylcholine-stimulated ^{22}*Na$^+$ influx and* ^{125}*I-labeled α-toxin binding*

Effects of simultaneous or 30 min prior decidium exposure. Inhibition data were obtained as described under "Experimental Procedures" and in Fig. 1. Data were analyzed as described by Sine and Taylor, 1979. Values are given ±S.D. and the number of determinations are in parentheses.

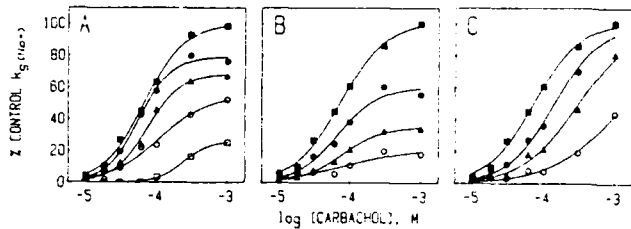| AcChR source and exposure duration	K_p (M) (^{22}Na$^+$ influx)	n_H	K_p (M) (^{125}I-labeled α-toxin)	n_H
Intact BC3H-1 cells				
30 min	$1.2 \pm 0.5 \times 10^{-7}$	0.92 ± 0.18 (4)	$3.6 \pm 0.8 \times 10^{-7}$	0.69 ± 0.01 (3)
Instantaneous	$3.5 \pm 1.0 \times 10^{-7}$	0.66 ± 0.07 (4)	$5.0 \pm 0.7 \times 10^{-7}$	0.66 ± 0.07 (3)
Torpedo membranes				
30 min			$1.9 \pm 0.2 \times 10^{-7}$	0.73 ± 0.03 (3)
Instantaneous			$3.3 \pm 0.5 \times 10^{-7}$	0.77 ± 0.01 (3)

FIG. 2. **Antagonist inhibition of concentration-dependent carbamylcholine elicited Na^+ permeability in BC3H-1 cells.** $^{22}Na^+$ permeability elicited by the specified concentrations of carbamylcholine plus antagonist was measured over a 20-s interval in sets of culture dishes. Results are expressed as percent of the maximum rate in the absence of antagonist. *A*, decidium: ■——■, no added decidium; ●——●, 10^{-7} M; ▲——▲, 3×10^{-7} M; ○——○, 10^{-6} M; □——□, 3×10^{-6} M. *B*, dinaphthyldecamethonium: ■——■, no added dinaphthyldecamethonium; ●——●, 6×10^{-7} M; ▲——▲, 3×10^{-6} M; ○——○, 10^{-5} M. *C*, *d*-tubocurarine: ■——■, no added *d*-tubocurarine; ●——●, 3×10^{-7} M; ▲——▲, 10^{-6} M; ○——○, 6×10^{-6} M.

curarine, by contrast, shifts the curve to higher agonist concentrations without altering the maximal permeability response (Fig. 2C).

Decidium Enhancement of Agonist Competition with α-Toxin Binding—The previous data do not distinguish whether decidium converts AcChR to a state of increased agonist affinity and decreased functional responsiveness by association at the agonist site or at heterotropic, allosteric site(s). If decidium action was exerted solely at the agonist site, then decidium enhancement of the apparent agonist affinity should occur over the same concentration range as decidium competition with ^{125}I-labeled α-toxin binding. Alternatively, if decidium converts the AcChR to a state of increased agonist affinity by an allosteric mechanism as has been demonstrated for the noncompetitive inhibitors (Sine and Taylor, 1980; Boyd and Cohen, 1980; Quast *et al.*, 1978; Weiland *et al.*, 1976), we should observe a separation between the concentration dependences for direct decidium competition and allosteric enhancement of agonist competition with α-toxin binding. To address this question, we examined the concentration dependence for decidium augmentation of the competition of agonist with the initial rate of ^{125}I-labeled α-toxin binding, and these results were compared to the concentration dependence for decidium competition of the initial rate of ^{125}I-labeled α-toxin binding. Data on *Torpedo* membranes (Fig. 3A) and BC3H-1 cells (Fig. 3B) show identical decidium concentration dependences for inhibition of α-toxin binding and for augmentation of the competition of carbamylcholine with α-toxin binding. For comparison, Fig. 3C shows the corresponding result obtained with the local anesthetic meproadifen in *Torpedo* membranes. Here, meproadifen enhances carbamylcholine competition with α-toxin binding at far lower concentrations than those required for inhibition of α-toxin binding.

Decidium Modulation of [³H]PCP Binding—[³H]PCP has been shown previously to bind selectively to a site on the receptor which is noncompetitive with and allosterically coupled to agonist binding (Albuquerque *et al.*, 1980; Heidmann *et al.*, 1983). Prolonged occupancy by agonists and certain antagonists converts the receptor to a desensitized state exhibiting increased agonist affinity as well as increased affinity for noncompetitive inhibitors such as PCP. Occupancy of the agonist site by α-toxin prevents the conversion of the receptor to the desensitized state. Conversely, occupancy of the noncompetitive inhibitor site by PCP converts the receptor to a state exhibiting increased affinity for certain agonists (Palma *et al.*, 1986). We, therefore, examined the influence of decidium on [³H]PCP binding to the *Torpedo* AcChR in the
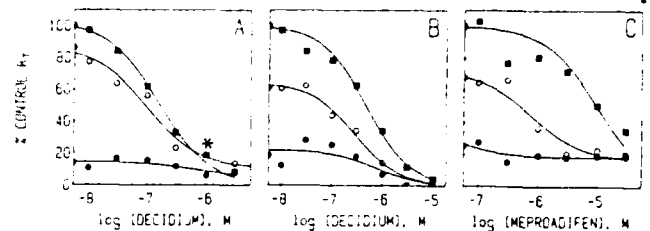
FIG. 3. **Decidium and meproadifen enhancement of carbamylcholine competition with the initial rate of ^{125}I-labeled α-toxin binding to AcChR in *Torpedo* membranes and BC3H-1 cells.** Decidium and meproadifen were added in the specified concentrations 30 min before initiating the toxin-binding reaction. Carbamylcholine was added either 10 s or 30 min before addition of α-toxin. Initial rates of toxin binding were measured over 40 s and expressed as a percent of the rate observed in the absence of added effector. ○——○, rate of binding measured with 10 s of prior exposure to agonist; ●——●, rate of binding with 30 min of prior exposure to agonist; ■——■, rate of binding with exposure only to decidium or meproadifen. *A*, decidium, *Torpedo* membranes. ED_{50} for 10 s, 30 min, and no exposure to carbamylcholine were 0.10, 0.60, and 0.16 μM, respectively. The test carbamylcholine concentration was 1 μM. *B*, decidium, BC3H-1 cells. ED_{50} for 10 s, 30 min, and no exposure to carbamylcholine were 0.29, 0.74, and 0.47 μM, respectively. The test carbamylcholine concentration was 30 μM. *C*, meproadifen, *Torpedo* membranes. ED_{50} for 10 s, 30 min, and no exposure to carbamylcholine were 0.79, 0.03, and 1.0 μM, respectively. The test carbamylcholine concentration was 1 μM. *Asterisk* indicates overlapping data points.
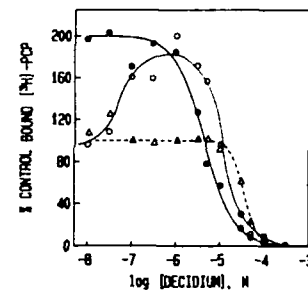

FIG. 4. **Decidium modulation of [³H]PCP binding to the *Torpedo* membranes.** Assays solutions contained membranes (1.0 μM in α-toxin sites), [³H]PCP (1.0 μM), plus specified effector ligand concentrations. ●——●, in the presence of carbamylcholine (200 μM); △——△, in the presence of α-toxin (10 μM); ○——○, in the absence of both α-toxin and carbamylcholine.

absence and presence of excess carbamylcholine or α-toxin (Fig. 4). A subsaturating concentration of [³H]PCP was used in order to monitor both increases or decreases in the capacity of [³H]PCP to bind to the AcChR.

When the agonist sites are occupied with saturating concentrations of carbamylcholine or α-toxin increasing concentrations of decidium displace [³H]PCP, consistent with direct action of decidium at the noncompetitive inhibitor site in its high and low affinity states, respectively. As expected, carbamylcholine alone enhances the fraction of bound [³H]PCP. Using previously determined values for the K_d of PCP toward the desensitized and resting receptor states, the K_d of decidium toward the site in these two states were calculated to be 1.2 and 29 μM, respectively.

In the absence of either carbamylcholine or α-toxin, decidium exhibits biphasic effects on [³H]PCP binding (Fig. 4). Low concentrations of decidium increase [³H]PCP binding to the level observed in the presence of carbamylcholine, suggesting that decidium interaction at the agonist site converts the receptor to a state exhibiting increased [³H]PCP binding. At higher concentrations decidium inhibits [³H]PCP binding, indicating decidium directly competes with the PCP-binding site.

Spectroscopic Characterization of Decidium-AcChR Complexes—Excitation and emission fluorescence spectra of decidium complexed with the agonist and high affinity noncompetitive inhibitor sites were obtained either in the presence of excess PCP, to block the noncompetitive inhibitor site, or excess carbamylcholine, to block the agonist site. Contributions to the spectra arising from free ligand and light scatter were subtracted to yield the difference spectra. The corrected excitation maximum of decidium complexed with the agonist site appears at 490 nm, while the excitation maximum of decidium at the noncompetitive inhibitor site appears at 530 nm (Fig. 5A). The fluorescence emission maximum of decidium complexed to the agonist or the high affinity noncompetitive inhibitor sites appear between 605 and 610 nm (Fig. 5B). The apparent quantum yield of decidium increases about 2-fold upon binding to either the agonist or the noncompetitive inhibitor sites.

Fluorescence Titrations—Equilibrium binding parameters for decidium association at the agonist sites were determined by fluorescence titrations (Fig. 6). Excitation at 290 nm was used to maximize the signal from the bound fluorophore. The spectral overlap between receptor tryptophanyl emission and decidium absorbance in the 340-nm band results in substantial enhancement of the bound decidium signal relative to 480 nm of excitation. All samples contained 100 μM PCP to prevent decidium binding to the noncompetitive inhibitor site. Fig. 6B shows the specific fluorescence from decidium bound to the agonist sites, where nonspecific binding was defined using excess cobra α-toxin. In four replicate titrations we obtained composite values of $K_d = 0.57 \pm 0.34$ μM and $n_H = 0.89 \pm 0.19$.

The observation of a Hill coefficient less than unity suggested nonequivalence of decidium dissociation constants at the agonist sites. We also carried out displacement titrations of decidium by the agonist carbamylcholine, which displays a unitary Hill coefficient for binding (Weiland *et al.*, 1977) (Fig. 7). At saturation, carbamylcholine reduces decidium fluorescence to a similar extent as excess α-toxin. Hill analysis of the data (Fig. 7B) reveal $n_H = 0.85$. The observation of Hill coefficients less than unity for displacement of decidium further suggests some nonequivalence for the interaction of

decidium at the agonist sites, in accord with the pharmacological studies. Analogous results were obtained by competition with the partial agonist decamethonium (data not shown).

Energy Transfer between FITC-toxin and Decidium—To examine the distance between the two agonist sites on the individual receptor molecules, we assessed dipolar fluorescence energy transfer between FITC-toxin and decidium bound to the agonist sites on the receptor. Doubly liganded receptors were prepared to achieve the fractional occupation described under "Experimental Procedures." Saturating concentrations of PCP were added to prevent decidium binding to the noncompetitive inhibitor site. The spectral overlap integral between FITC emission and decidium excitation, J, was calculated to be 2.49×10^{-14} cm$^3 \cdot$M^{-1} (*cf.* Fig. 4 and data not shown). Assuming a refractive index of 1.4 and an orientation factor (κ^2) of 0.67, R_0 was calculated to be 30Å.

Various factors render quantitation of steady-state energy transfer between FITC-toxin and decidium bound to the AcChR difficult. These factors include the significant overlap of decidium and FITC emission spectra and the innerfilter effects of decidium at the FITC absorption maxima. Since fluorescence lifetimes are unaffected by innerfilter effects and since an appropriate combination of interference filters could be chosen which reduces the contribution of decidium fluorescence to less than 5% of the FITC fluorescence signal, we have chosen to determine energy transfer as the extent of reduction of donor FITC fluorescence lifetime (Equation 4) in the presence of the acceptor decidium. The results of studies on membrane-associated and detergent-solubilized receptor preparations are presented in Fig. 8 and Table II. In the absence of added decidium and with 15% occupancy by FITC-toxin, the exponential decay of FITC-toxin fluorescence was satisfactorily described by a single fluorescence lifetime ($\tau = 3.9$ ns). When decidium was added to saturate the remaining agonist sites, a 16% decrease was observed in the fluorescence lifetime of FITC-toxin bound to the membrane-associated AcChR (Fig. 8A). This quenching was not altered by the further addition of native α-toxin (Fig. 8B) and was abolished by solubilizing the receptor with cholate (Fig. 8, C and D). Taken together, the reduction in FITC-toxin fluorescence
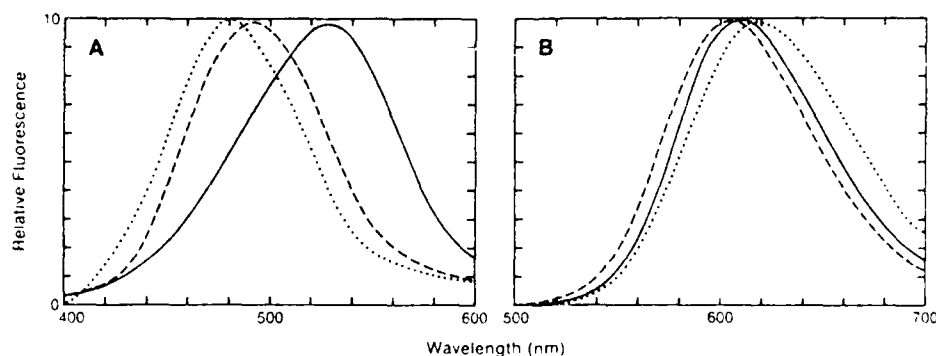

Wavelength (nm)

FIG. 5. *A*, normalized and corrected difference excitation spectrum of decidium bound to the enriched AcChR membranes. *Dashed line* represents the difference spectrum for decidium bound to the agonist sites obtained from samples (AcChR, 0.25 μM in α-toxin sites; decidium, 1.0 μM; PCP, 100 μM) in the absence and presence of carbamylcholine (500 μM). *Solid line* represents difference spectrum for decidium bound to the noncompetitive inhibitor site obtained from samples (AcChR, 1.0 μM in α-toxin sites; decidium, 2.0 μM; carbamylcholine, 500 μM) in the absence and presence of PCP (100 μM). *Dotted line* represents the corrected emission spectrum of decidium in buffer. *B*, normalized uncorrected difference emission spectrum of decidium bound to the membrane-enriched AcChR. *Dashed line* represents the difference spectrum for decidium bound to the agonist sites obtained from samples (AcChR, 0.25 μM in toxin sites; decidium, 1.0 μM; PCP, 100 μM) in the absence and presence of carbamylcholine (500 μM). *Solid line* represents difference spectrum for decidium bound to the noncompetitive inhibitor site obtained from samples (AcChR, 1.0 μM in toxin sites; decidium, 2.0 μM; carbamylcholine, 500 μM) in the absence and presence of PCP (100 μM). *Dotted line* represents the uncorrected excitation spectrum of decidium in buffer.
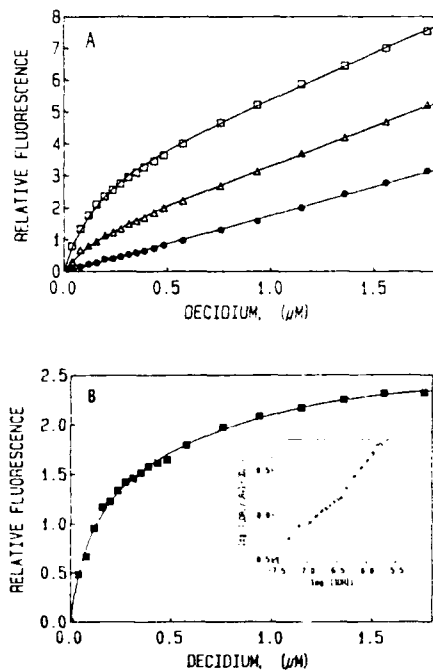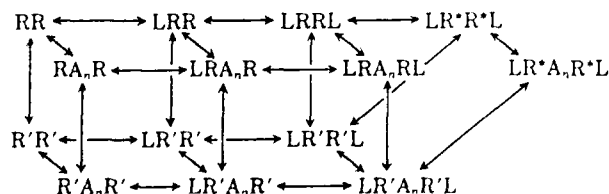
FIG. 6. *A*, titration of membrane-enriched AcChR with decidium. Incremental quantities of decidium were added to 2.0 ml of membrane suspension of AcChR (0.2 µM in α-toxin sites) and 100 µM PCP. Fluorescence was measured at 620 nm with excitation at 290 and corrections made for dilution and inner filter effects. □——□, membranes in the absence of α-toxin; △——△, membranes in the presence of 2 µM α-toxin to define nonspecific binding; ●——●, buffer only. *B*, plot of specific enhancement of fluorescence as percentage of receptor bound *versus* the concentration of free ligand. The *inset* represents a Hill plot of this data.

FIG. 7. **Displacement titration of the decidium-AcChR complex by carbamylcholine.** *Panel A*, decidium (2.5 µM) and PCP (100 µM) were equilibrated with receptor-enriched membranes (0.25 µM in α-toxin sites). Incremental quantities of carbamylcholine were then added. Data were corrected for nonspecific fluorescence determined in a companion titration in the presence of excess α-toxin. *Panel B*, plot of the data shown in *panel A* according to Equation 1. *f*, *f_B*, and *f_C* represent the observed fluorescence, fluorescence with decidium alone, and fluorescence in presence of excess competing ligand. [*D*] and [*C*] are the estimated free concentrations of decidium and competing ligand, respectively.

lifetime does not stem from decidium at the agonist site or nonspecifically associated with the receptor molecule but reflects energy transfer between FITC-toxin bound to the agonist site and decidium partitioned nonspecifically into the lipid bilayer. If we assume a detection limit of 5% transfer between agonist sites, then Equation 2 predicts a minimum separation between fluorophores at the agonist sites of $1.63 \times R_0$, or 49 Å. Hence, the greater than 49 Å separation between the agonist sites is too distant to produce the reduction in lifetime of FITC-labeled toxin in the presence of decidium. The minimal but measurable excitation transfer efficiency indicates that at high concentrations decidium can partition into the membrane.

DISCUSSION

The dynamics of the nicotinic AcChR function have been extensively studied from several perspectives (Karlin, 1980; Adams, 1981; Taylor *et al.*, 1983; Changeux *et al.*, 1984). Within the timescale in which our studies are conducted, the AcChR can be thought to exist in equilibrium between at least three types of states: resting (R), activated (R*), and desensitized (R′) (Scheme I). Additional transient desensitized states have been shown to exist but after equilibrium exposure a single desensitized state is presumed to predominate.
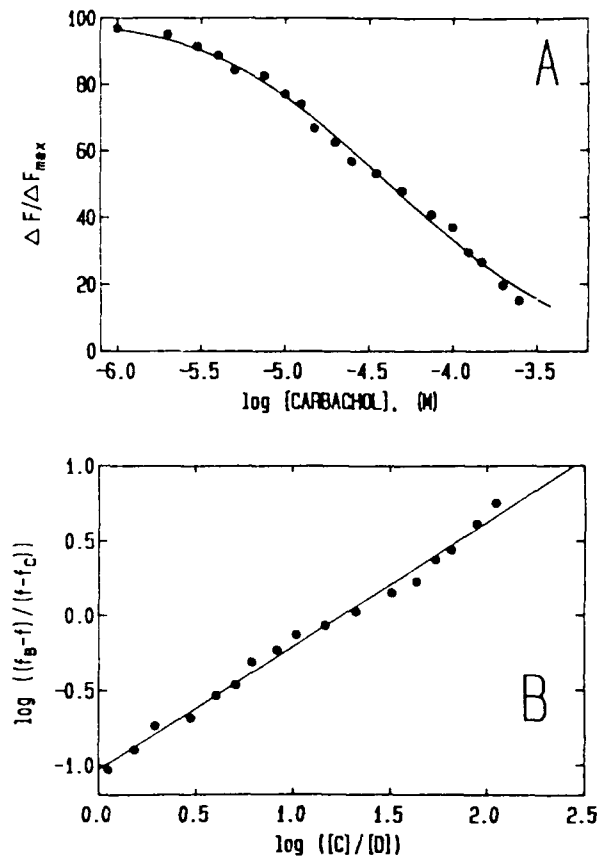

SCHEME 1

Changes in the population distribution of receptor molecules between these states govern the functional and binding properties of the receptor. In the absence of agonist (L) or noncompetitive inhibitor (A), the receptor exists predominantly in the activatible state (RR), exhibiting a comparatively low agonist affinity. Agonists bind to receptor, activate the cation channel, and concomitantly but more slowly convert the receptor to a desensitized state. The desensitized states display higher agonist binding affinity and no receptor-mediated cation permeability. The preference of a ligand for binding to the desensitized receptor is the driving force underlying desensitization.

Agents which perturb receptor functional responses may do so by competitive or noncompetitive mechanisms. Classical antagonists inhibit agonist-stimulated cation fluxes by direct competition at the agonist-binding sites (Neubig and Cohen, 1979), exhibit little or no preference for the R′R′ relative to RR states and do not effect transitions to the active state (Sine and Taylor, 1981). A large and heterogeneous class of inhibitors noncompetitively inhibit channel opening by agonists. Most, but not all, of these noncompetitive inhibitors enhance the conversion of receptor to a desensitized state. Typical of such agents are the local anesthetics, general anesthetics, PCP, and certain toxins such as histrionicotoxin. Certain antagonists competitively inhibit agonist activation and in addition convert the receptor to a desensitized state.

FIG. 8. Decidium quenching the fluorescence lifetime of FITC-toxin bound to the AcChR. Nanosecond decay curves of FITC-toxin (0.6 μM) were recorded in the presence of AcChR (4 μM in α-toxin sites), decidium (10 μM), and PCP (100 μM). The timing calibration was 0.43 ns/channel. *Dashed lines represent the lamp pulse. Deviations of the experimental data points from a single exponential theoretical function (solid lines) are shown in the upper curves.* AcChR is membrane-associated in *panels A* and *B* and solubilized with 4% cholate in *panels C* and *D*. In *panels B* and *D* native α-toxin (10 μM) was incubated with the AcChR 30 min after the addition of FITC-toxin to inhibit decidium binding to the agonist sites. Decidium was added to the sample cuvettes just before initiating the 1-h data accumulation period. The data accumulation interval was limited to 1 h in order to minimize the displacement of FITC-toxin from the agonist sites by decidium. The apparent decay curves generated from samples that did not contain FITC-toxin were subtracted from the AcChR samples to correct for light scatter.
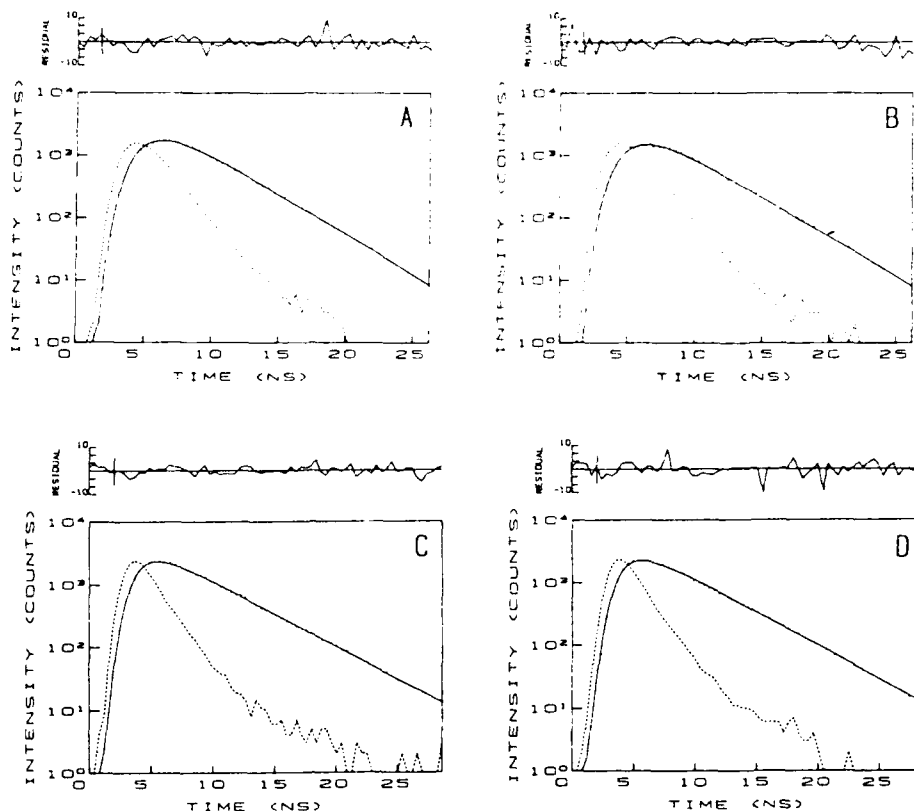

TABLE II

Nanosecond fluorescence decay (ex:450 and em:520 nm) of FITC-toxin bound to the AcChR (membrane-enriched and solubilized at 4.0μM in α-toxin sites) in the presence and absence of decidium (10 μM)

PCP (100 μM) was present to block binding to the noncompetitive inhibitor site for PCP. In each case sufficient FITC-toxin (0.6 μM) was added to occupy 15% of the vacant sites. This decidium concentration (10 μM) should yield ~93% occupancy of the vacant sites.

	Lifetimes in ns $\pm$ S.D. (No. of determinations)	
	Solubilized	Membrane-enriched
FITC-toxin + AcChR	3.9 ± 0.1 (2)	3.8 ± 0.1 (2)
FITC-toxin + decidium + AcChR	3.8 ± 0.1 (3)	3.2 ± 0.2 (4)
FITC-toxin + α-toxin + decidium + AcChR	3.8 ± 0.1 (3)	3.2 ± 0.2 (4)

Classical pharmacologic studies distinguish these agents as metaphilic antagonists (Rang and Ritter, 1970a, 1970b). Metaphilic antagonists exhibit higher affinity for the desensitized state of the receptor and therefore show a greater capacity to block the permeability response after exposure to carbamylcholine. The actions of decidium are consistent with it exhibiting metaphilic properties. Decidium exhibits mixed competitive and noncompetitive inhibition of agonist-stimulated ^{22}Na$^+$ influx (Fig. 2). Equilibrium exposure of the receptor to decidium converts the receptor to a state exhibiting increased decidium binding affinity (Fig. 1 and Table I). Decidium binding to the agonist site enhances [^{3}H]PCP binding to an allosterically coupled noncompetitive site (Fig. 4). Decidium by itself does not stimulate ^{22}Na$^+$ influx in BC3H-1 cells, so it is not a partial agonist. Hence, these results indicate that upon occupation of the agonist sites decidium converts the AcChR to a functionally blocked state toward which agonists and noncompetitive inhibitors display a higher affinity. In addition to its functional antagonism and ability to convert the receptor to a high affinity state by occupying the agonist

sites, decidium at higher concentrations binds directly to the PCP-binding site (Fig. 4).

Fluorescence characterization of decidium bound to the two classes of binding sites indicates significant shifts in both the excitation and emission spectra, which are consistent with an environment of greater hydrophobicity upon binding to the AcChR. A red-shift in the excitation spectrum of far greater magnitude is associated with decidium binding to the noncompetitive site (~50 nm) than to the agonist sites (~10 nm). This suggests that the noncompetitive site for PCP is more hydrophobic than the agonist-binding sites, *i.e.* in a domain less susceptible to solvent proton transfer from the excited singlet state (Olmstead and Kearns, 1977).

In a previous study of the interaction of ethidium with the AcChR, we observed that this phenylphenanthridium ligand binds selectively to the noncompetitive inhibitor site for PCP, particularly when the receptor is in a desensitized state (K_d ~ 0.4 μM) (Herz *et al.*, 1987). Like decidium, ethidium displays a large red-shift in the excitation (~47 nm) and a blue-shift in the emission (~35 nm) maxima upon binding to the noncompetitive inhibitor site for PCP. These results also show that a portion of the binding domain of the noncompetitive site is particularly hydrophobic. Furthermore, addition of a second quaternary group separated by 10 methylene groups dramatically changes the relative binding selectivity of these phenylphenanthridium congeners for the two respective sites.

Fluorescence titrations confirm that functional antagonism by low concentrations of decidium occurs via occupation of the agonist site and that decidium binds nonequivalently to the two agonist sites on the receptor oligomer, although the degree of nonequivalence is small relative to antagonists such as pancuronium or dimethyl-*d*-tubocurarine. Studies on reversible (Weiland *et al.*, 1976; Sine and Taylor, 1981; Neubig and Cohen, 1979) and site-directed irreversible antagonists (Damle and Karlin, 1978) also show nonequivalence of the sites. Despite the identity in the sequence of the α subunits (Noda *et al.*, 1982) differential post-translational glycosylation has been reported (Ratnam *et al.*, 1986). Thus, either the

differential glycosylation or the lack of identity of subunits neighboring the α-subunit could be responsible for the nonequivalence in binding sites.

To measure distances between the two agonist sites on the receptor, we estimated the efficiency of excitation energy transfer between a slowly reversible α-toxin and a highly reversible ligand, decidium. We observed no energy transfer between the FITC-toxin and the decidium when each is bound to one of the two agonist sites on doubly liganded receptors. Previous studies using a hybrid receptor-fluorescent-α-toxin complex, where FITC-toxin is on one of the subunits and tetramethylrhodamine-toxin occupies the other subunit, exhibit inter*subunit* and inter*receptor* transfer in the membrane-associated receptor and intersubunit transfer in the solubilized receptor (Johnson et al., 1984). Intersubunit excitation transfer measurements afforded a distance of 67 Å (range 55–84 Å) between the fluorophores conjugated to lysine 23 of the α-toxin, consistent with location of these lysine 23-conjugated fluorophores at the outer perimeter of the 85–90 Å diameter receptor molecule. However, interpretation of these data was limited by uncertainty in the location of the fluorophore relative to the orientation of bound α-toxin molecule. Although the α-carbon of lysine 23 is no more than 19 Å away from any other α-carbon in the α-toxin, the α-toxin molecule is an asymmetric, peptide ($M_r = 7820$) with dimensions of 20 × 30 × 40 Å (Walkinshaw et al., 1980). The absence of energy transfer between lysine 23-FITC-toxin and decidium in the present study confirms our previous estimate of the intersite distance measured between fluorophores conjugated at lysine 23 on the two α-toxin molecules. With a critical transfer distance of 30 Å for fluorescein to decidium, 5% transfer of energy will occur at 49 Å. This value is significantly less than the 67 Å measured between fluorophores for the two fluorescent α-toxins. If the agonist sites where decidium binds are located on the extracellular surface near the pseudo-axis of symmetry, then energy transfer should have been observed. The absence of detectable energy transfer confirms our previous suggestion that the agonist sites reside at a distance from rather than near the pseudo-axis of symmetry of the receptor. Our findings are consistent with previous suggestions that the central loop of the α-toxin, which contains lysine 23, overlies the agonist site. Thus, energy transfer studies with decidium have allowed us to place further constraints on the location of the agonist sites when ligands are associated with the receptor.

While no site-specific energy transfer was detected between the decidium and FITC-toxin specifically bound to the agonist sites, minimal dipolar transfer efficiency (16%) can be detected between FITC-toxin and decidium associated nonspecifically with the lipid or the receptor molecule. Decidium has sufficient hydrophobicity to partition into the lipid bilayer. Since we also found no energy transfer with the solubilized receptor, the membrane itself is the likely site of nonspecific decidium association. Due to uncertainty in the donor-acceptor stoichiometry, precise estimates of distance between the agonist site and the lipid bilayer can not be obtained. Never-

theless, our results suggest proximity of the agonist-binding sites to the lipid bilayer, which is consistent with the recent finding the Cys-192 and Cys-193 are proximal to both the acetylcholine-binding site and the beginning of the proposed M1 membrane spanning hydrophobic region (Ile-210) of the α subunit (Kao et al., 1984).

REFERENCES

Adams, P. R. (1981) *J. Membr. Biol.* **58**, 161–174
Albuquerque, E. X., Tsai, M-C., Aronstan, R., Witkop, B., Eldefrawi, A. T., and Eldefrawi, M. E. (1980) *Mol. Pharmacol.* **18**, 159–178
Berman, H. A., Decker, M. M., Nowak, M. W., Leonard, K. J., McCauley, M., Baker, W., and Taylor, P. (1987) *Mol. Pharmacol.*, in press
Bolger, M. B., Dionne, V., Chrivia, J., Johnson, D. A., and Taylor, P. (1984) *Mol. Pharmacol.* **26**, 57–69.
Boyd, N. D., and Cohen, J. B. (1980) *Biochemistry* **19**, 5344–5353
Brown, R. D., and Taylor, P. (1983) *Mol. Pharmacol.* **23**, 8–16
Changeux, J.-P., Devillers-Thiery, A., and Chemouilli, P. (1984) *Science* **224**, 1335–1345
Damle, V. N., and Karlin, A. (1978) *Biochemistry* **17**, 2039–2045
Forster, T. (1959) *Discuss. Faraday Soc.* **27**, 7–17
Forster, T. (1965) in *Modern Quantum Chemistry* (Sinanoglu, O., ed) (Part 3, pp. 93–137, Academic Press, New York
Heidmann, T., and Changeux, J.-P. (1979) *Eur. J. Biochem.* **94**, 255–279
Heidmann, T., and Oswald, R. E., and Changeux, J.-P. (1983) *Biochemistry* **22**, 3112–3127
Herz, J. M., Johnson, D. A., and Taylor, P. (1987) *J. Biol. Chem.* **262**, 7238–7247
Johnson, D. A., and Taylor, P. (1982) *J. Biol. Chem.* **257**, 5632–5636
Johnson, D. A., Voet, J. G., and Taylor, P. (1984) *J. Biol. Chem.* **259**, 5717–5725
Johnson, D. A., and Yguerabide, J. (1985) *Biophys. J.* **48**, 949–955
Kao, P. N., Dwork, A. J., Kaldany, R.-R. J., Silver, M. L., Wideman, J., Stein, S., and Karlin, A. (1984) *J. Biol. Chem.* **259**, 11662–11665
Karlin, A. (1980) in *The Cell Surface and Neuronal Function* (Poste, G., Nicolson, G. L., and C. W. Cotman, eds) pp. 141–260, Raven Press, New York
Karlsson, E., Arnberg, H., and Eaken, D. (1971) *Eur. J. Biochem.* **21**, 1–16
Munson, P. J., and Rodard, D. (1980) *Anal. Biochem.* **107**, 220–239
Noda, M., Takahashi, H., Tanabe, T., Toyosato, M., Furutani, Y., Hirose, T., Asai, M., Inayama, S., Miyata, T., and Numa, S. (1982) *Nature* **299**, 793–797
Neubig, R. R., Krodel, E. K., Boyd, N. D., and Cohen, J. B. (1979) *Proc. Natl. Acad. Sci. U. S. A.* **76**, 690–694
Neubig, R. R., and Cohen, J. B. (1979) *Biochemistry* **18**, 5464–5475
Olmstead, J., III, and Kearns, D. R. (1977) *Biochemistry* **16**, 3647–3654
Oswald, R. E., Heidmann, T., and Changeaux, J.-P. (1983) *Biochemistry* **22**, 3128–3136
Palma, A., Herz, J. M., Wang, H. H., and Taylor, P. (1986) *Mol. Pharmacol.* **30**, 243–251
Prinz, H., and Maelicke, A. (1983a) *J. Biol. Chem.* **258**, 10263–10271
Prinz, H., and Maelicke, A. (1983b) *J. Biol. Chem.* **258**, 10273–10282
Quast, U., Schimerlik, M., Lee, T., Witzemann, V., Blanchard, S., and Raftery, M. A. (1978) *Biochemistry* **17**, 2405–2414
Rang, H. P., and Ritter, J. M. (1970a) *Mol. Pharmacol.* **6**, 357–382
Rang, H. P., and Ritter, J. M. (1970b) *Mol. Pharmacol.* **6**, 383–390
Ratnam, M., Gullick, W., Spiess, J., Wan, W., Criado, M., and Lindstrom, J. (1986) *Biochemistry* **25**, 4268–4275
Reed, K., Vandlen, P., Bode, J., Duguid, J., and Raftery, M. A. (1975) *Arch. Biochem. Biophys.* **167**, 138–144
Schmidt, J., and Raftery, M. A. (1973) *Anal. Biochem.* **52**, 349–355
Sine, S. M., and Taylor, P. (1980) *J. Biol. Chem.* **255**, 10144–10156
Sine, S. M., and Taylor, P. (1981) *J. Biol. Chem.* **256**, 6692–6699
Tan, Y., and Barrantes, F. J. (1980) *Biochem. Biophys. Res. Commun.* **92**, 766–774
Taylor, P., and Lappi, S. (1975) *Biochemistry* **14**, 1989–1997
Taylor, P., Culver, P., Sine, S. M., and Johnson, D. A. (1983) in *The Biochemical Basis of Drug Action* (Singer, T. P., Mansour, T. E., and Ondarza, R. N., eds) pp. 9–25, Academic Press, New York
Walkinshaw, M. M., Saenger, W., and Maelicke, A. (1980) *Proc. Natl. Acad. Sci. U. S. A.* **77**, 2400–2404
Weiland, G. A., Georgia, B., Wee, V. T., Chign II, C. F., and Taylor, P. (1976) *Mol. Pharmacol.* **12**, 1091–1105
Weiland, G. A., Georgia, B., Lappi, S., Chignell, C. F., and Taylor, P. (1977) *J. Biol. Chem.* **252**, 7648–7656
Weiland, G. A., and Taylor, P. (1979) *Mol. Pharmacol.* **15**, 197–212
Yguerabide, J. (1972) *Methods Enzymol.* **26**, 498–578

Kinetic, Equilibrium, and Spectroscopic Studies on Dealkylation ("Aging") of Alkyl Organophosphonyl Acetylcholinesterase

ELECTROSTATIC CONTROL OF ENZYME TOPOGRAPHY*

Harvey Alan Berman and Mildred M. Decker

From the Department of Biochemical Pharmacology, State University of New York at Buffalo, Buffalo, New York 14260

The mechanism of dealkylation ("aging") of branched-alkyl organophosphonyl conjugates of acetylcholinesterase and the consequence of this reaction on enzyme conformation were examined by employing kinetic, equilibrium, and spectroscopic techniques. Aging of cycloheptyl methylphosphono-acetylcholinesterase proceeded as a unimolecular reaction in which the enzyme became refractory to oxime reactivation and was accelerated with increases in temperature and decreases in pH and ionic strength of the medium. While aging occurred in a manner invariant with the nature of the salt in buffers containing Na^+, K^+, Rb^+, Cs^+, Cl^-, CH_3COO^-, SO_4^{2-}, and PO_4^{3-}, the influence of ionic strength on aging was *opposite* to that predicted for a mechanism requiring charge separation during formation of the polar transition state. Examination of the equilibrium enzyme conformation with decidium, a fluorescent active center-selective ligand, revealed marked alterations in ligand association and a greater ionic strength dependence for binding after aging. The explanation for this behavior focuses on the high net negative surface charge of the enzyme and proposes that acetylcholinesterase topography is governed by the strength of electrostatic interactions between charged, contiguous, mobile protein regions within the subunit. As such, these studies reveal a reciprocal relationship between acetylcholinesterase topography, surface charge, and ionic strength of the medium.

Acetylcholinesterase is readily modified at the active center by a variety of organophosphates and organophosphonates (Froede and Wilson, 1971; Aldridge and Reiner, 1972). Reactions with branched-chain alkyl esters of organophosphorus agents form conjugates with AchE[1] which undergo a unimolecular reaction during which the conjugate, although still phosphonylated, becomes refractory to oxime reactivation (Fleisher and Harris, 1965; Coult *et al.*, 1966). The propensity for this process termed aging parallels carbonium ion stability of the branched alkyl substituent and hence is described as a dealkylation through alkyl-oxygen bond scission (Coult *et al.*,

[1] The abbreviations used are: AchE, acetylcholinesterase; MP-AchE, methylphosphono-acetylcholinesterase; decidium diiodide, 3,8-diamino-5,10'-(trimethylammonium)decyl-6-phenyl phenanthridinium diiodide; BisTris, 2-[bis(2-hydroxyethyl)amino]-2-(hydroxymethyl)-propane-1,3-diol.
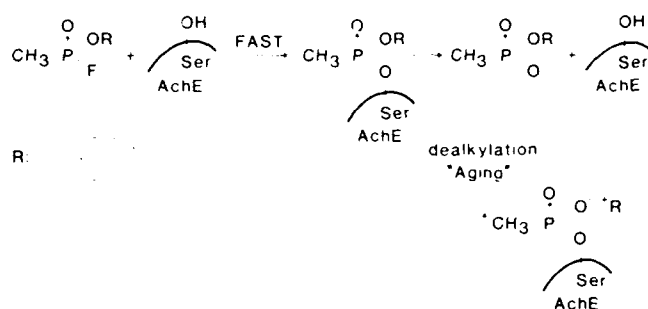
SCHEME 1

1966; Aldridge and Reiner, 1972; Froede and Wilson, 1971).

Scheme 1 illustrates these reactions for cycloheptyl methylphosphono-acetylcholinesterase which is formed from the reaction of cycloheptyl methylphosphonofluoridate with acetylcholinesterase. Upon dealkylation this conjugate loses the cycloheptyl moiety and is converted to methylphosphono-acetylcholinesterase (MP-AchE). Although this reaction is understood on the basis of a carbonium ion mechanism, there exists a paucity of information concerning the role played by the enzyme in stabilizing carbonium ion formation and promoting alkyl-oxygen bond scission.

To gain insight into the mechanism of aging and its consequences on acetylcholinesterase conformation, we have examined the dependence of aging kinetics on pH, ionic strength, temperature, and in the presence of site-specific cationic ligands known to alter enzyme conformation. Equilibrium binding and steady-state and time-correlated fluorescence spectroscopy are employed to examine the resulting conformation of the methylphosphono-enzyme obtained upon aging. In particular, the present study questions whether the changes induced upon aging are confined to the protein regions encompassed within the active center or extend to regions remote from the active center.

Advantage is taken of decidium (see Structures), a fluorescent bisquaternary phenanthridinium ligand that is a competitive inhibitor of substrate hydrolysis and ligand association at the active center, and as discerned from its ligand specificity exhibits binding modes similar to that of decamethonium.[2] Cycloheptyl methylphosphonofluoridate was chosen as the phosphonylating agent since the conjugate formed with acetylcholinesterase undergoes aging with a half-life of approximately 5 h and hence is readily measured under routine laboratory conditions (Benschop and Keijer, 1966).

EXPERIMENTAL PROCEDURES

Materials—Acetylcholinesterase from *Torpedo californica* (Pacific Biomarine, Venice, CA) was obtained by affinity chromatography of

[2] H. A. Berman *et al.*, manuscript in preparation.

Decidium

Phenyltrimethylammonium   Edrophonium
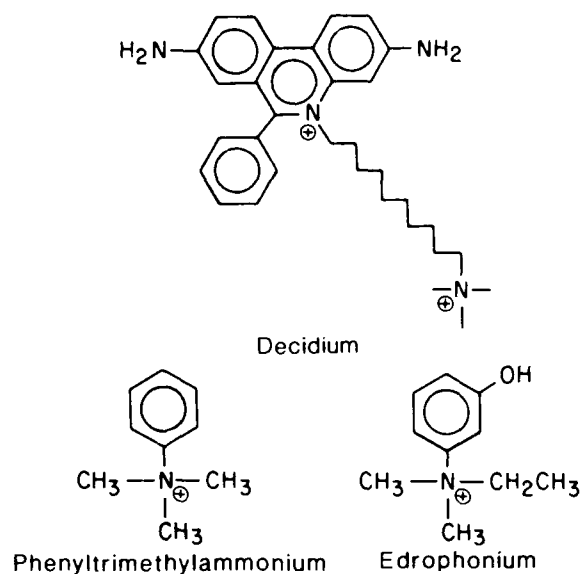
Structures of ligands used in this study.

electroplax homogenates subjected to light trypsin digestion (Taylor *et al.*, 1974). Cycloheptyl methylphosphonofluoridate was synthesized by reaction of cycloheptanol with methylphosphonodifluoridate according to published procedures (Benschop and Keijer, 1966) and the structure verified by proton nuclear magnetic resonance spectroscopy (*cf.* Berman *et al.*, 1985a).

Cycloheptyl methylphosphono-acetylcholinesterase was isolated from a Sephadex G-25 column following reaction of the enzyme with a 2-fold excess of the organophosphorus agent. Aging was allowed to proceed by incubation of the conjugate for 4 h at 37 °C, 4 h at 25 °C, followed by extensive dialysis at 4 °C. Prior to study of the conjugate, a sample of enzyme was withdrawn and tested for completion of aging in the presence of TMB-4 (1 mM). The buffer medium was a 0.01 N Tris-Cl buffer, pH 8.0, containing 0.1 N NaCl and 0.04 M MgCl$_2$.

Acetylcholinesterase concentrations were assessed from the UV spectrum at 280 nm by employing the extinction coefficient of $c_{280}^{1\%}$ = 17.5 (Taylor *et al.*, 1974). The extinction coefficient for methylphosphono-acetylcholinesterase was determined relative to that for the native enzyme by comparing its UV absorption spectrum with the protein concentration determined with fluorescamine as a protein detection agent (Dohlen *et al.*, 1973). AchE in the range of 5-50 μg served as the protein standard. The extinction coefficient for MP-AchE was determined to be 20.3 ± 1.3 and was 15-20% greater than the value for AchE.

Decidium diiodide (m.p. 166-177 °C) was synthesized employing the reaction sequence described by Watkins (1952) and Walls (1947). Synthesis and characterization of decidium will be published elsewhere.[3] Concentrations of solutions of decidium were calculated from the intensity of its absorption spectrum at 480 nm, ϵ = 6000 M^{-1} cm^{-1}.

Propidium diiodide (Behring Diagnostics), gallamine triethiodide (K and K Chemicals), d-tubocurarine (Sigma), rubidium chloride (GFS Chemical Co.), cesium chloride (optical grade; Sigma), and *N*-methylacridinium (Molecular Probes, Inc.) were used without further purification. Edrophonium chloride was a gift from Hoffmann-La Roche. The *n*-alkyl trimethylammonium ligands, present as iodide (C$_2$, C$_4$, C$_5$, C$_6$) or as bromide (C$_8$, C$_{10}$, C$_{12}$) salts, and the bisquaternary polymethonium ligands, present as bromide salts, were gifts from Professor David J. Triggle, School of Pharmacy, State University of New York at Buffalo.

Catalytic Measurements—AchE activity was measured on a Radiometer TTT-60 autoburette titrator operated in the pH-stat mode. The reaction volume was 20 ml, and enzyme activity was measured against 0.5 mM acetylcholine chloride after a 200-1000-fold dilution of enzyme. The Ellman procedure (Ellman *et al.*, 1961) for the hydrolysis of acetylthiocholine in the presence of 5,5'-dithiobis(2-nitrobenzoic acid) was employed as an alternative measure of acetylcholinesterase activity.

Spectroscopy—UV spectra were obtained on Beckman UV/vis 25 and Cary 210 spectrophotometers. Fluorescence titrations were conducted on an Aminco-Bowman Ratio II spectrofluorometer. Corrected excitation and emission fluorescence spectra were obtained on a SPEX 212 system.

Time-correlated fluorescence lifetime measurements were obtained on a lifetime system from PRA (London, Ontario). The excitation and emission wavelengths for measurement of propidium and decidium decay rates were selected with a monochromator on the excitation side and sharp cut-on filters (KV590 Schott) on the emission side. Data were deconvoluted for the finite duration of the lamp pulse by employing the nonlinear regression procedure of Grinvald and Steinberg (1974). When more than one lifetime component was present, the weighted average lifetime was expressed as follows,

$$<\tau> = \Sigma a_i \tau_i / \Sigma a_i$$

where a and τ denote the amplitude and lifetime, respectively, of component i (Yguerabide, 1972).

Determination of Aging Rate Constants—Cycloheptyl methylphosphono-acetylcholinesterase was obtained by reaction of AchE with a 2-fold excess of cycloheptyl methylphosphonofluoridate and isolated by passage through a Sephadex G-25 column. The progress of gel filtration was monitored by measuring the absorption of the protein at 280 nm with an ISCO UV scanner. Labeled enzyme appeared in the void volume and was collected and diluted with the appropriate buffer to achieve the desired pH, ionic strength, and enzyme concentration. A typical procedure for inhibition and isolation required approximately 10 min. Aging was monitored as the loss of capacity to recover AchE activity in the presence of TMB-4 (1 mM). The kinetic profile was assessed at different times after inhibition by removing samples of the reaction mixture and allowing them to incubate in the presence of oxime for approximately 12 reactivation half-lives (20 h) prior to measurement of enzyme activity.

Competitive Dissociation of Decidium—In a typical competitive titration the enzyme was present at an initial concentration of 3 × 10^{-7} M in subunit sites. Decidium was present at concentrations greater than 16-fold the dissociation constant and at least 2 times the stoichiometry of binding sites. These conditions obviate consideration of the uncomplexed sites, and the dissociation constant for nonfluorescent ligands can be obtained from the following relationship, $(F_0 - F)/(F - F_c) = (K_F/K_C)[C]/[F]$, where F_0 denotes the initial fluorescence intensity when all sites are saturated with decidium, F_c the fluorescence when all sites are saturated with competitor, and F the fluorescence measured in the presence of the nonfluorescent competitive ligand. C and F represent the concentration of the nonfluorescent competitive ligand and decidium, respectively. Logarithmic plots of $(F_0 - F)/F - F_c)$ *versus* $[C]/[F]$ give a slope of unity for a homogeneous class of independent sites. The value of the competitor dissociation constant, K_C, is obtained from the x intercept and the known value of the decidium dissociation constant, K_F (Berman *et al.*, 1981; Taylor and Lappi, 1975).

RESULTS

Aging of cycloheptyl methylphosphono-acetylcholinesterase was monitored by measuring the capacity for reactivation of the organophosphonyl conjugate in the presence of TMB-4 (1 mM). When measured at 25 °C, pH 8.0, in buffer containing 0.1 N NaCl and 0.04 M MgCl$_2$, reactivation of this conjugate occurred at a rate of 0.4 h^{-1} and if initiated within 10 min of inhibition proceeded to greater than 90% completion. The extent of oxime-induced restoration of enzyme activity diminished in an exponential manner with a rate constant of 0.17 ± 0.05 h^{-1}, a value similar to that obtained by Benschop and Keijer (1966). The exponential time course for aging of cycloheptyl methylphosphono-AchE was consistent with the reaction occurring within a single homogeneous class of reactive sites.

Influence of Ionic Strength and pH on Aging Kinetics—Upon transfer of cycloheptyl methylphosphono-acetylcholinesterase from buffers (pH 8.0) containing 0.45 N NaCl to those containing 0.01 N NaCl, rates of aging increased from 0.095 ± 0.009 to 0.47 ± 0.02 h^{-1}, respectively (Fig. 1). Aging rates were dependent on sodium chloride concentration and varied 8-fold over the range of concentrations examined. In the presence of RbCl and CsCl (Fig. 1), aging rate constants
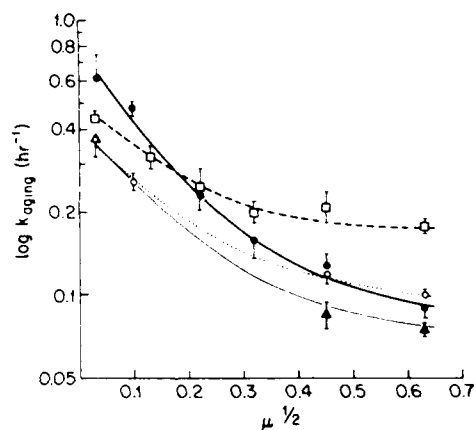
FIG. 1. **Dependence of aging of cycloheptyl methylphos-phono-acetylcholinesterase on ionic strength of the medium.**
The rate constants for aging of cycloheptyl methylphosphono-acetyl-cholinesterase are plotted against ionic strength ($\mu^{1/2}$) of the buffer medium. Aging of cycloheptyl methylphosphono-acetylcholinester-ase was measured in a 0.01 N Tris-Cl buffer, pH 8.0, in the presence of different concentrations of NaCl, KCl, RbCl, or CsCl. The *heavy solid line* (●——●) presents the dependence of aging rate, k_{aging}, on concentration of NaCl, and is compared with results obtained for aging in buffers containing KCl (□- - -□), RbCl (○····○), and CsCl (▲——▲). The data for NaCl and KCl are the average ± S.E. of at least four determinations, whereas those for RbCl and CsCl are the average ± S.E. of at least 2 determinations.

were within 1.2-fold of those observed in the presence of NaCl. In the presence of KCl concentrations less than 0.1 M aging rates were within the range of values observed for the other alkaline salts; at concentrations greater than 0.1 M aging occurred approximately 2-fold faster than when meas-ured in the presence of NaCl. Aging rate constants determined in the presence of sodium salts of CH_3COO^- (0.13 ± 0.02), SO_4^{2-} (0.12 ± 0.04), and PO_4^{3-} (0.16 ± 0.02 h^{-1}) at an ionic strength of 0.1 M were indistinguishable from those deter-mined in the presence of Cl^- (0.16 ± 0.03 h^{-1}). Hence, specific salt effects were absent, and aging kinetics were governed by ionic strength of the medium.

Fig. 2 presents the relationship between aging rate con-stants measured over the range pH 4–8 in buffers of high (0.45 N) and low (0.05 and 0.01 N NaCl) ionic strengths. In all buffers a decrease in pH resulted in an increase in aging rate. In the presence of 0.45 N NaCl, the rate *versus* pH profile between the values pH 4.75–8.0 was sigmoid and characterized by a midpoint of pH 6.1. Although the inherent error at low pH allowed for only poor discrimination between different mechanisms of general acid catalysis, the pH dependence did not conform to the Henderson-Hasselbalch equation for ion-ization of a single enzymic group (Fig. 2, *inset*) and, hence, it was not correct to assign the midpoint value of this profile to a pK_a of a single enzymic residue.

The pH-rate profiles obtained for aging at 0.05 and 0.01 N NaCl ionic strength were shifted approximately 0.3–0.4 pH unit to alkaline regions. In low ionic strength buffers of pH less than 4.75 there was a marked deceleration of aging as noted also by Schoene *et al.* (1980). Under these conditions, however, the rapid rate of aging precluded precise determi-nation of kinetic rate constants.

Temperature Dependence of Aging—The rate of aging in-creased with increases in temperature and over the range 4–37 C obeyed the Arrhenius equation. From a plot of log K_{aging} *versus* $1/T$ for the data obtained at 4 °C (5 ± 1 × 10⁻³), 15 °C (0.03 ± 0.01), 25 C (0.17 ± 0.05), 30 °C (0.36 ± 0.03), and 37 C (0.74 ± 0.21 h^{-1}), the activation energy was calculated to be 25.6 kcal/mol, a value which was 10 kcal/mol greater
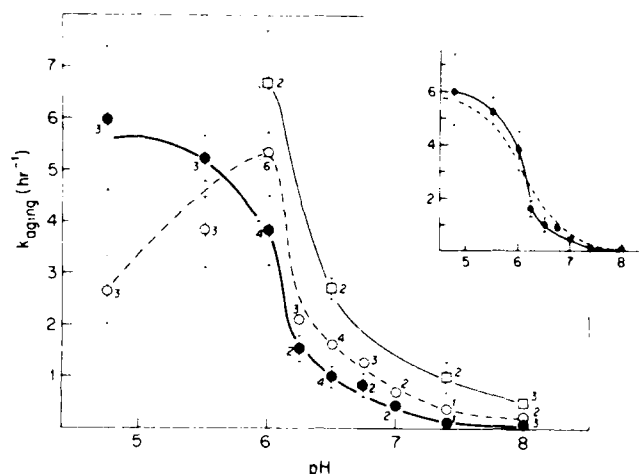

FIG. 2. **Dependence of aging of cycloheptyl methylphos-phono-acetylcholinesterase on pH and ionic strength of the reaction medium.** Aging was determined in buffers of different pH containing 0.45 N NaCl (●——●), 0.05 N NaCl (○- - -○), and 0.01 N NaCl (□——□). The data are presented as the average ± the S.E. over the numbers of determinations denoted above the data points. The following buffers were employed: pH 4.0–5.5, sodium acetate (0.01 N); pH 6.0–7.0, BisTris (0.05 M); pH 7.0–8.0, Tris-Cl (0.01 N). *Inset*, comparison of the pH-rate data obtained in buffer of 0.45 N ionic strength with that calculated for ionization of a single group at the enzyme surface employing the equation $k_{app} = k_i/[1 + (K_a/H^+)]$ (Mahler and Cordes, 1971). The observed aging rate constant, k_{app}, was calculated by employing a value of 6 h^{-1} for k_i, the maximal rate constant observed, and 6.1 as an estimate for pK_a, the ionization constant derived from the midpoint of the pH dependence.

than that reported for aging of bovine erythrocyte AchE in pH 7.4 buffers of physiologic ionic strength (Keijer *et al.*, 1974).

Influence of Site-specific Cations—Aging kinetics deter-mined in the presence of four classes of cationic ligands were independent of ligand concentrations greater than 10-fold their dissociation constants. In the presence of edrophonium and N-methylacridinium, cations specific for the active center (Taylor and Lappi, 1975; Mooser and Sigman, 1974; Rosen-berry and Neumann, 1977), and gallamine, d-tubocurarine, and propidium, ligands selective for the peripheral anionic site (Taylor and Lappi, 1975; Berman *et al.*, 1981), aging occurred at rates that were within 2-fold of that observed in the absence of ligand (Table I) and were similar to effects reported by Schoene (1978) and Crone (1974). In the presence of the polymethonium bisquaternary ligands hexamethonium and decamethonium, ligands which bind in a mutually exclu-sive manner with cation association at both the peripheral and active center sites (Berman *et al.*, 1980), aging occurred 7–8.5 times more slowly than in the absence of ligands. The corresponding monoquaternary hexyl- and decyltrimeth-ylammonium cations, in contrast, exerted only negligible in-fluence on aging.

Spectroscopic Characterization of Decidium Complexes with Acetylcholinesterase and Methylphosphono-acetylcholinester-ase—Association of decidium with acetylcholinesterase and methylphosphono-acetylcholinesterase resulted in a shift of the absorption spectrum from 480 nm, the value seen in buffer, to 505 nm. The band position and extinction coeffi-cients of the decidium absorption spectra for complexes with AchE and MP-AchE were identical.

Excitation spectra of decidium complexes with AchE and MP-AchE showed maxima at 505 nm, in agreement with the absorption spectra. The emission maxima of the complexes were blue-shifted to 610 nm from the value of 645 nm observed

for the ligand in buffer. Although the position and bandwidth were identical, the integrated quantum yield of the native complex was approximately 50% greater than that of the aged complex. The ratio of the fluorescence lifetime of the complex with AchE (11 ns) and that with the aged conjugate (6 ns) were in excellent agreement with the ratio of the steady-state quantum yields, thereby indicating the absence of any static quenching (Yguerabide, 1972).

Association of propidium with AchE and MP-AchE resulted in a blue-shift of the fluorescence maxima to 630 nm from the value of 662 nm observed for the ligand free in buffer. In contrast to the case for decidium, the positions, bandshapes, and integrated intensities of the propidium emission spectra of the native and aged proteins were equivalent.

TABLE I

The influence of cationic ligands on aging kinetics of cycloheptyl methylphosphono-acetylcholinesterase

Reaction kinetics were determined at 25 °C, in a 0.01 N Tris-Cl buffer, pH 8.0, containing 0.1 N NaCl and 0.04 M $MgCl_2$. In a typical determinaton, AchE was present at concentrations of $1-3 \times 10^{-6}$ M in subunit sites. Ligands were present at concentrations at least 10-fold their dissociation constants (Taylor and Lappi, 1975; Berman *et al.*, 1981; or as determined in this study, Table II). Values reported represent the average ± S.E. of at least two determinations.

Ligand	k	Control/ligand
	$h^{-1} \times 10^{2}$	
Control	17 ± 5	1
Edrophonium	11 ± 2	1.5
N-Methylacridinium	7.4 ± 0.1	2.3
Gallamine	6.4 ± 0.3	2.6
d-Tubocurarine	7.5 ± 0.2	2.2
Decamethonium	2.4 ± 0.3	7.1
Hexamethonium	2.0 ± 0.5	8.5
Decyltrimethylammonium	11 ± 3	1.5
Hexyltrimethylammonium	17 ± 4	1

Association of Decidium and Propidium with Acetylcholinesterase and Methylphosphono-acetylcholinesterase—Association of decidium with AchE and MP-AchE was monitored by enhancement of the ligand fluorescence at 610 nm upon excitation at 535 nm. The equilibrium titration profile obtained for association of decidium with MP-AchE was saturable and compatible with a stoichiometry of one ligand bound per 80,000-dalton subunit. From a Scatchard plot of these data a dissociation constant was calculated to be $1.4 \pm 0.5 \times 10^{-8}$ M and was comparable with the value found for decidium association with AchE ($K_D = 2.1 \pm 0.2 \times 10^{-8}$ M). The affinities of propidium for AchE and MP-AchE (Table II) were within 2-fold of each other.

Competitive Dissociation of Bound Decidium—The relationship between dissociation constant and chain length of bisquaternary polymethonium ligands containing 6-10 methylene groups interposed between the cationic termini and n-alkyl monoquaternary trimethylammonium ligands containing 5-12 methylene groups is presented in Figs. 3 and 4, respectively. Affinity of each enzyme form for bisquaternary ligands increased with increasing chain length, while a more complex relationship was observed for the monoquaternary ligands. The *insets* in Figs. 3 and 4 present the relative changes in affinity of the bisquaternary and n-alkyl monoquaternary ligands for methylphosphono-acetylcholinesterase with respect to acetylcholinesterase. For bisquaternary ligands the relative affinities were 1-4-fold higher with MP-AchE than with AchE and *increased with increasing ligand chain length* (Fig. 3). For monoquaternary ligands the relative affinities were 1-4-fold higher with MP-AchE than with AchE and *increased with decreasing ligand chain length* (Fig. 4).

Dissociation constants obtained for active center selective ligands are reported in Table II. N-Methylacridinium exhibited equivalent affinity for MP-AchE and AchE; the values obtained were independent of whether association of the ligand was determined directly through measurement of its fluorescence or indirectly through its capacity to dissociate
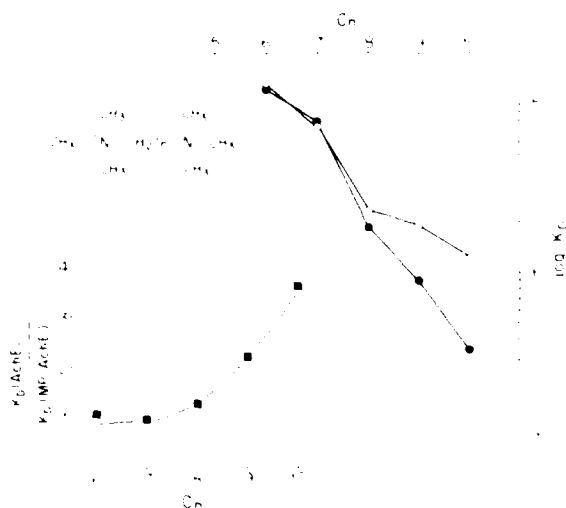
TABLE II

Dissociation constants determined for cationic ligands with native and methylphosphonyl forms of acetylcholinesterase

The dissociation constants for propidium and decidium were determined from direct measurement of their fluorescence at 610 nm upon excitation at 535 nm. The values for the other ligands were determined from their capacity to dissociate either decidium (A) or propidium (B), employing the appropriate dissociation constant.

Ligand	K_D			$K_D(AchE)/K_D(MP\text{-}AchE)$
	AchE	MP-AchE	Ψ-MP-AchE	
		M		
A. High ionic strength[a]				
Decidium	$2.1 \pm 0.2 \times 10^{-8}$	$1.4 \pm 0.5 \times 10^{-8}$	$2.4 \pm 0.7 \times 10^{-8}$	1.5
Propidium	3×10^{-6} [b]	$2 \pm 1 \times 10^{-6}$	$5.2 \pm 0.6 \times 10^{-6}$	1.5
Edrophonium	$2.0 \pm 0.1 \times 10^{-7}$	$2.6 \pm 1.1 \times 10^{-5}$	$5.9 \pm 0.4 \times 10^{-5}$	0.01
Phenyltrimethylammonium	$1.6 \pm 0.1 \times 10^{-5}$	$7.9 \pm 0.5 \times 10^{-5}$		0.2
N-Methylacridinium	$7.3 \pm 2.9 \times 10^{-8}$	$6.9 \pm 0.8 \times 10^{-8}$		1.1
	$1.2 \pm 0.5 \times 10^{-7}$ [c]	$6.5 \pm 1.1 \times 10^{-8}$		1.8
Decamethonium	$1.2 \pm 0.1 \times 10^{-6}$	$3.4 \pm 0.7 \times 10^{-7}$	$7.1 \pm 0.4 \times 10^{-7}$	3.5
B. Low ionic strength[d]				
Propidium	1×10^{-7}	$1.6 \pm 0.5 \times 10^{-8}$		6
Gallamine	$0.7 \pm 0.3 \times 10^{-7}$ [e]	$1 \pm 0.4 \times 10^{-8}$		7
Hexamethonium	$5.3 \pm 1.9 \times 10^{-6}$	$3.2 \pm 0.4 \times 10^{-7}$		16
Octamethonium	$1.3 \pm 0.3 \times 10^{-6}$	$3.0 \pm 0.1 \times 10^{-8}$		44
Decamethonium	$2.3 \pm 0.7 \times 10^{-7}$	$3.0 \pm 0.5 \times 10^{-9}$		76

[a] The titrations were carried out in a 0.01 N Tris-Cl buffer, pH 8.0, containing 0.1 N NaCl and 0.04 M $MgCl_2$, by measuring the capacity of the nonfluorescent ligands to dissociate decidium.

[b] Values taken from Taylor and Lappi (1975).

[c] Derived from direct measurement of N-methylacridinium fluorescence at 490 nm upon excitation at 360 nm.

[d] The titrations were carried out in a 0.001 N Tris-Cl buffer, pH 8.0, by measuring the capacity of the nonfluorescent ligands to dissociate propidium.

[e] Taken from Berman *et al.* (1981).

FIG. 3. **Relationship between chain length of bisquaternary polymethonium ligands and affinity with acetylcholinesterase and methylphosphono-acetylcholinesterase.** Dissociation constants were estimated from the ligand capacity to dissociate complexes of decidium and AchE (○——○) and MP-AchE (●——●). The reaction medium was a 0.01 N Tris-Cl buffer, pH 8.0, at 25 °C, containing 0.1 N NaCl and 0.04 M MgCl₂. *Inset*, relationship between the relative increase in ligand affinity and chain length.
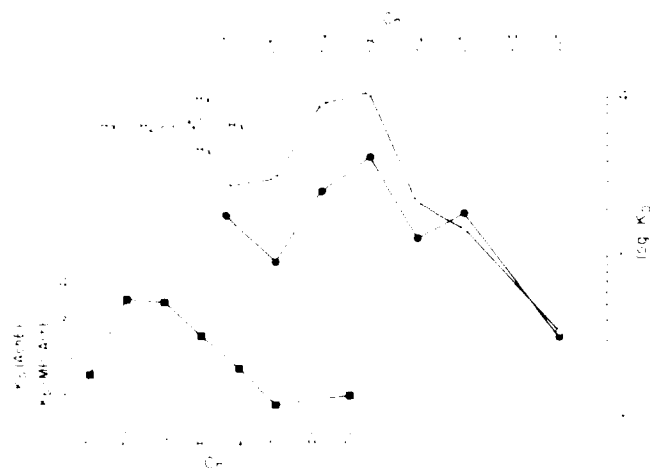

FIG. 4. **Relationship between chain length of *n*-alkyl trimethylammonium ligands and affinity with acetylcholinesterase and methylphosphono-acetylcholinesterase.** Dissociation constants were estimated from the ligand capacity to dissociate complexes of decidium with AchE (———) and MP-AchE (●——●). The reaction medium was a 0.01 N Tris-Cl buffer, pH 8.0, at 25 °C, containing 0.1 N NaCl and 0.04 M MgCl₂. *Inset*, relationship between the relative increase in ligand affinity and chain length.

decidium. Phenyltrimethylammonium and edrophonium exhibited 5- and 130-fold lower affinities for the aged enzyme relative to the native enzyme, respectively.

Although the dissociation constants observed for the *n*-alkyl mono- and bisquaternary ligands as estimated from their capacities to dissociate decidium were smaller than the inhibition constants observed by Belleau (Belleau *et al.*, 1965; Belleau and DiTullio, 1970) and Bergmann and Segal (1954) in early studies with bovine erythrocyte enzyme, the relationships between K_D, K_I, and chain length were in qualitative agreement. It is noteworthy that the values of the dissociation constants determined for decamethonium and edrophonium with AchE were compatible with their capacities to inhibit hydrolysis of cationic substrates (Mooser and Sigman, 1974; Taylor and Lappi, 1975).

SCHEME 2
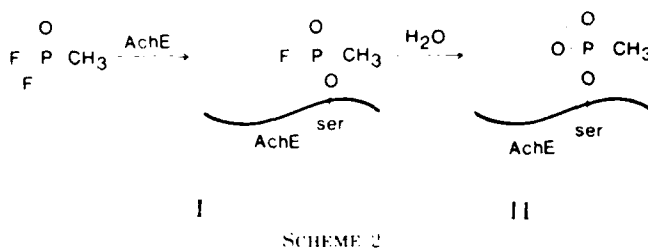
Influence of Ionic Strength on Ligand Affinity—The influence of ionic strength on ligand affinity for AchE and MP-AchE was examined in a low ionic strength (0.001 N) Tris-Cl buffer, pH 8.0, in the absence of salt (Table IIB). Propidium and gallamine exhibited 6–7-fold higher affinities for the aged relative to the native enzyme. As estimated from their capacities to dissociate propidium complexes in a low ionic strength buffer, hexamethonium, octamethonium, and decamethonium showed, respectively, 16-, 44-, and 76-fold greater affinities for MP-AchE relative to AchE.

Association of Cationic Ligands with Pseudo-methylphosphono-acetylcholinesterase—The influence of a negative charge within the serine containing region of the active center was examined by measuring ligand association with a phosphonylated form of the enzyme that arises without enzymic aging (Scheme 2). Methylphosphonodifluoridate inhibits AchE to form fluoromethylphosphono-AchE (*I*) which upon reaction with H₂O decomposes to form a conjugate, designated Ψ-MP-AchE (*II*), that is isoelectric with the aged conjugate. Decidium, propidium, edrophonium, and decamethonium exhibited affinities for Ψ-MP-AchE that were within 2-fold of those found for MP-AchE (Table II).

DISCUSSION

Carbonium Ion Mechanism of Aging—The rates of aging of branched-alkyl organophosphonyl conjugates of acetylcholinesterase are known to parallel carbonium ion stability and support a mechanism in which the rate-limiting step is alkyl-oxygen bond scission (*cf.* Scheme 1; Benschop and Keijer, 1966; Smith and Usdin, 1966). The salient features of a carbonium mechanism are the *charge separation* developed during the transition state and the role played by *charge delocalization* in accelerating bond scission. As discussed by Warshel (1981), electrostatic stabilization of the incipient carbonium ion formed during lysozyme hydrolysis of polysaccharides facilitates formation of the polar transition state by approximately 6–8 kcal/mol relative to the corresponding hydrolysis in water. The activation energy of 25.6 kcal/mol found for dealkylation of cycloheptyl methylphosphono-acetylcholinesterase is comparable with those values ($E_a \sim$ 20–25 kcal/mol) found for solvolysis of the corresponding cycloalkyl and benzyl tosylates (Roberts and Chambers, 1951; Fang *et al.*, 1958; Kochi and Hammond, 1953; Benschop and Keijer, 1966), thereby indicating that apposition of the phosphonyl ester moiety with the active center confers no apparent reduction in the activation barrier for dealkylation.

The ionic strength dependence observed for aging of cycloheptyl methylphosphono-acetylcholinesterase (Fig. 1) is *opposite* to that predicted for a mechanism requiring substantial charge delocalization during the transition state (Moore and Pearson, 1981; Bender *et al.*, 1984). The modest shift of approximately 0.3–0.4 pH unit in the aging rate *versus* pH profile (Fig. 2) is far smaller than the displacement of 1.6 pH units observed upon transfer of AchE from buffers of high (0.1 N) to low (0.006 N NaCl) ionic strength (Hofer *et al.*, 1984; see also Douzou and Maurel, 1977; Voet *et al.*, 1981).

Hence, the observed dependence of aging on ionic strength is not compatible with a direct influence of ionic strength on polarization of the scissile bond and implicates a mechanism mediated through an indirect influence on enzyme conformation.

The synergistic inhibition of aging seen in the presence of hexa- and decamethonium but not ligands selective for the active center and peripheral anionic sites (Table I) indicates that the restrictions on bond scission reflect a characteristic binding mode of the bisquaternary polymethonium ligands. The active center and peripheral anionic sites are topographically distinct loci separated by more than 25 Å (Berman *et al.*, 1980) and appear to be associated with highly mobile protein segments (Berman *et al.*, 1985b). Since bisquaternary polymethonium ligands bind in a mutually exclusive manner with ligand occupation of these sites, the reduced rates of alkyl-oxygen cleavage can arise from a restriction in the motional freedom imposed by cross-linking the corresponding protein segments.

Electrostatic Relationships on the Acetylcholinesterase Surface—Since ligand association with Ψ-MP-AchE is identical with that of MP-AchE, aging-induced alterations in ligand association can be attributed to the presence of a negative charge in the esteratic region of the active center irrespective of the mechanism of charge formation. By employing a simple model of single point charges immersed in a continuous medium of dielectric constant ϵ, the free energy (ΔG) governing interaction of oppositely charged species of Z_+ and Z_- valences, carrying e^+ and e^- units of charge, can be estimated from the equation describing Bjerrum ion association theory, $\Delta G = Z_+ Z_- e^+ e^- / a\epsilon$, where a is the interionic distance (Moore and Pearson, 1981). If the active center is considered to contain −6 units of charge (Nolte *et al.*, 1980), then formation of an additional unit of negative charge upon dealkylation would favor ligand association by a ratio of 7/6, leading to a predicted 3-fold enhancement in ligand affinity. Although only a crude approximation the predicted 3-fold enhancement in ligand affinity for MP-AchE is not incompatible with some of the results observed for the structurally different classes of ligand (Table II, Figs. 3 and 4).

Topographic Relationships on the Acetylcholinesterase Surface—A proposal based solely on the strength of electrostatic interaction between a ligand and a distinct site, however, does not afford an adequate explanation for the dramatic reduction in edrophonium affinity following aging of the enzyme. The AchE complex with the hydroxyl-containing edrophonium but not phenyltrimethylammonium gains stability through hydrogen bonding with an acceptor residue within the active center (Changeux, 1966). The 130-fold reduction in edrophonium affinity after aging of acetylcholinesterase, representing a 2.8 kcal/mol reduction in binding energy, falls within the range estimated for the hydrogen bond contribution to complex stabilization between ligand and protein (Fersht *et al.*, 1985) and, compared with the modest 5-fold reduction in phenyltrimethylammonium affinity and the near equivalence in affinity of these structurally related ligands after enzyme aging, is not incompatible with loss of a hydrogen bond contribution to complex stabilization.

Nor does such a proposal account for the increasing stabilization of complex formation with MP-AchE relative to AchE with *increasing* chain length of bisquaternary ligands (Fig. 3) and *decreasing* chain length of monoquaternary ligands (Fig. 4). Since the chain length dependences arise primarily from changes in entropy reflecting corresponding changes in the water-alkane and water-protein interactions, the higher ligand affinities of the mono- and bisquaternary ligands for

MP-AchE appear to signify the higher degree of solvation of the *n*-alkyl-binding crevice on the aged conjugate relative to the native enzyme (*cf.* Belleau and DiTullio, 1970; Bolger and Taylor, 1979).

Finally, comparison of the data in Table II and Fig. 3 reveals that transfer of methylphosphono-acetylcholinesterase from buffers of high to low ionic strength results in 38-, 62-, and 113-fold increases in enzyme affinity for hexa-, octa-, and decamethonium, respectively. Similar transfer of acetylcholinesterase results in only 1 5-fold increases in affinity for bisquaternary ligands. Hence, ligand association with the aged conjugate exhibits a markedly greater sensitivity than with the native enzyme to changes in ionic strength of the medium.

Electrostatic Control of Acetylcholinesterase Topography—One explanation for this kinetic and equilibrium behavior proposes that the spatial relationship between distinct sites on the AchE subunit is highly variable and by virtue of the enzyme's high net negative charge is governed by mutual repulsive interactions between contiguous like-charged protein segments (Fig. 5). In this view, Coulombic repulsion between the negatively charged methylphosphono-serine residue and the anionic subsite results in expansion of the active center beyond the equilibrium dimensions characteristic of the native enzyme, leading to increased solvation of the enzyme surface. If we consider these two sites as point charges separated by a minimal distance of 4.7 Å (Froede and Wilson, 1971) and immersed in a high dielectric medium such as water, then the electrostatic interaction energy driving any such protein deformation is calculated to be approximately 0.8 kcal/mol. Although the distance separating these sites likely is greater than 4.7 Å, the electrostatic interaction energy
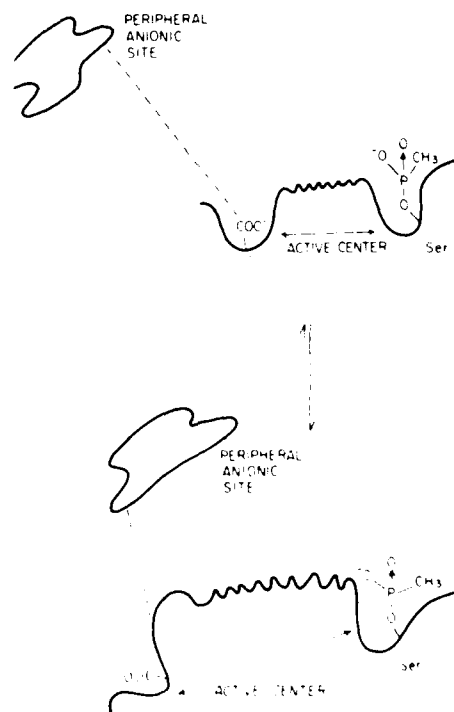

FIG. 5. **Proposal describing electrostatic relationships between active center and peripheral anionic site on the acetylcholinesterase subunit.** The *upper* and *lower views* illustrate, respectively, the equilibrium spatial relationship between the peripheral anionic site and the active center prior to and following swelling of the active center after aging. Distortion of the protein region encompassing the active center through Coulombic repulsion between the net negative methylphosphonoserine residue and the anionic subsite relieves electrostatic destabilization and, in turn, alters enzyme topography and protein solvation.

for protein deformation is predicted to be amplified by the presence of more than 1, and likely at least 6, effective negative charges estimated to exist within the active center (Nolte *et al.*, 1980), as well as an active center dielectric constant lower than that of the aqueous medium (Berman and Taylor, 1978; Amitai *et al.*, 1982). This proposal formally resembles the mechanism proposed for energy storage through charge separation in bacteriorhodopsin (Honig *et al.*, 1979) and is reminiscent of the expansion or unfolding of proteins that occurs after chemical modification of the protein surface charge (Habeeb *et al.*, 1958; Valenzuela and Bender, 1971; Spomer and Wootton, 1971).

Such a proposal provides a physical basis for the ionic strength dependence of dealkylation. Expansion or swelling of the net negative active center upon transfer of the enzyme *from buffers of high to low ionic strength facilitates access of* the bulk aqueous medium to the scissile bond, thereby promoting charge delocalization and faster rates of bond scission. On the basis of this mechanism, steric orientation of the scissile bond within the active center is concluded to play a role of little importance in governing the capacity for aging. The comparatively high activation energy for bond scission supports this conclusion, as do reports that aging of diasteriomeric conjugates formed from reaction of acetylcholinesterase with 2-methyl-*n*-heptyl- and pinocolyl methylphosphonates are invariant with chiral orientation about the epimeric α-carbon of the scissile alkyl-oxygen bond (Keijer and Wolring, 1969; de Jong and Wolring, 1984). While we have no unequivocal explanation for nonconformity of the pH dependence with the Henderson-Hasselbalch equation, the data seem to suggest the occurrence of more than a single ionization and, as such, afford an insufficient basis for identifying *a distinct amino acid residue responsible for proton transfer* to the scissile alkyl-oxygen bond. Hence, the active center appears to merely provide a reaction cage, the physical characteristics of which, microscopic pH and dielectric constant, govern the kinetics for bond scission.

Spectroscopic Analysis of Aged and Native Acetylcholinesterase The spectroscopic studies of decidium complexes support these conclusions. One mechanism governing quantum yields and lifetimes of phenanthridinium ligands focuses on the diffusion-limited capacity for excited-state proton transfer (Olmstead and Kearns, 1977). Any factor which serves to reduce the rates of proton transfer, such as occlusion of the ligand from contact with the bulk protic medium, serves to enhance the quantum efficiency and fluorescence lifetime. Since decidium associates with the trimethylammonium moiety anchored within the active center and the phenanthridinium moiety extended toward the peripheral anionic site, *the reduction in decidium quantum yield and lifetime* indicates that the phenanthridinium binding environment on MP-AchE experiences greater accessibility to the bulk aqueous medium than on the native enzyme. The comparable fluorescence lifetimes of the propidium complex with AchE and MP-AchE indicate that the peripheral anionic site exhibits near equivalence on both enzyme forms. The capacity of the acetylcholinesterase subunit to undergo facile deformations in topography without concomitant alterations in physically remote sites and the reciprocal relationship between enzyme topography, net surface charge, and ionic strength of the medium implicates the presence of separate mobile domains (*cf.* Berman *et al.*, 1985b) and a prominent role for electrostatic control of acetylcholinesterase conformation.

REFERENCES

Aldridge, W. N., and Reiner, E. (1972) *Enzyme Inhibitors as Substrates*, North Holland Publishing Co., Amsterdam

Amitai, G., Ashani, Y., Gafni, A., and Silman, I. (1982) *Biochemistry* **21**, 2060 2069

Belleau, B., and DiTullio, V. (1970) *J. Am. Chem. Soc.* **92**, 6320 6325

Belleau, B., Tani, H., and Lie, F. (1965) *J. Am. Chem. Soc.* **87**, 2283 2285

Bender, M. L., Bergeron, R. J., and Komiyama, M. (1984) *The Bioorganic Chemistry of Enzymatic Catalysis*, Chapter 2, John Wiley & Sons, New York

Benschop, H. P., and Keijer, J. H. (1966) *Biochim. Biophys. Acta* **128**, 586 588

Bergmann, F., and Segal, R. (1954) *Biochem. J.* **58**, 692 698

Berman, H. A., and Taylor, P. (1978) *Biochemistry* **17**, 1704 1713

Berman, H. A., Yguerabide, J., and Taylor, P. (1980) *Biochemistry* **19**, 2226 2235

Berman, H. A., Becktel, W., and Taylor, P. (1981) *Biochemistry* **20**, 4803 4810

Berman, H. A., Olshefski, D. F., Gilbert, M., and Decker, M. M. (1985a) *J. Biol. Chem.* **260**, 3462 3468

Berman, H. A., Yguerabide, J., and Taylor, P. (1985b) *Biochemistry* **24**, 7140 7147

Bolger, M. B., and Taylor, P. (1979) *Biochemistry* **18**, 3622 3629

Changeux, J. P. (1966) *Mol. Pharmacol.* **2**, 369 392

Coult, D. B., Marsh, D. J., and Read, G. (1966) *Biochem. J.* **98**, 869 873

Crone, H. D. (1974) *Biochem. Pharmacol.* **23**, 460 463

Dohlen, P., Stein, S., Dairman, W., and Udenfriend, S. (1973) *Arch. Biochem. Biophys.* **155**, 213 220

Douzou, P., and Maurel, P. (1977) *Trends Biochem. Sci.* **2**, 14 17

Ellman, G. L., Courtney, K. D., Andres, V., Jr., and Featherstone, R. M. (1961) *Biochem. Pharmacol.* **7**, 88 95

de Jong, L. P. A., and Wolring, G. Z. (1984) *Biochem. Pharmacol.* **33**, 1119 1125

Fang, F. T., Kochi, J. K., and Hammond, G. S. (1958) *J. Am. Chem. Soc.* **80**, 563 568

Fersht, A. R., Shi, J.-P., Knill-Jones, J., Lowe, D. M., Wilkinson, A. J., Blow, D. M., Brick, P., Carter, P., Waye, M. M. Y., and Winter, G. (1985) *Nature* **314**, 235 238

Fleisher, J. H., and Harris, L. W. (1965) *Biochem. Pharmacol.* **14**, 641 650

Froede, H. C., and Wilson, I. B. (1971) in *The Enzymes* (Boyer, P. D., ed) 3rd Ed., Vol. 5, pp. 87 114, Academic Press, Orlando, FL

Grinvald, A., and Steinberg, I. Z. (1974) *Anal. Biochem.* **59**, 583

Habeeb, A. F. S. A., Cassidy, H. G., and Singer, S. J. (1958) *Biochim. Biophys. Acta* **29**, 587 593

Hofer, P., Fringeli, U. P., and Hopff, W. H. (1984) *Biochemistry* **23**, 2730 2734

Honig, B., Ebrey, T., Callender, R. H., Dinur, U., and Ottolenghi, M. (1979) *Proc. Natl. Acad. Sci. U. S. A.* **76**, 2503 2507

Keijer, J. H., and Wolring, G. Z. (1969) *Biochim. Biophys. Acta* **185**, 465 468

Keijer, J. H., Wolring, G. Z., and de Jong, L. P. A. (1974) *Biochim. Biophys. Acta* **334**, 146 155

Kochi, J. K., and Hammond, G. S. (1953) *J. Am. Chem. Soc.* **75**, 3445 3451

Mahler, H. R., and Cordes, E. H. (1971) *Biological Chemistry*, 2nd Ed., Chapter 2, Harper and Row, Publishers, Hagerstown, MD

Moore, J. W., and Pearson, R. G. (1981) *Kinetics and Mechanism*, Chapter 7, John Wiley & Sons, New York

Mooser, G., and Sigman, D. S. (1974) *Biochemistry* **13**, 2299 2307

Nolte, H.-J., Rosenberry, T. L., and Neumann, E. (1980) *Biochemistry* **19**, 3705 3711

Olmstead, J., III, and Kearns, D. R. (1977) *Biochemistry* **16**, 3647 3654

Roberts, J. D., and Chambers, V. C. (1951) *J. Am. Chem. Soc.* **73**, 5034 5040

Rosenberry, T. L., and Neumann, E. (1977) *Biochemistry* **16**, 3870 3878

Schoene, K. (1978) *Biochim. Biophys. Acta* **525**, 468 471

Schoene, K., Steinhaus, J., and Wertman, A. (1980) *Biochim. Biophys. Acta* **616**, 384 388

Smith, T. E., and Usdin, E. (1966) *Biochemistry* **5**, 2914 2918

Spomer, W. E., and Wootton, J. F. (1971) *Biochim. Biophys. Acta* **235**, 164 171

Taylor, P., and Lappi, S. (1975) *Biochemistry* **14**, 1989 1997

Taylor, P., Jones, J. W., and Jacobs, N. M. (1974) *Mol. Pharmacol.* **10**, 78 92

Valenzuela, P., and Bender, M. L. (1971) *Biochim. Biophys. Acta* **250**, 538 548

Voet, J. G., Coe, J., Epstein, J., Matossian, V., and Shipley, T. (1981) *Biochemistry* **20**, 7182 7185

Walls, L. P. (1947) *J. Chem. Soc. (Lond.)* 67 74

Warshel, A. (1981) *Accts. Chem. Res.* **14**, 284 290

Watkins, T. I. (1952) *J. Chem. Soc. (Lond.)* 3059 3064

Yguerabide, J. (1972) *Methods Enzymol.* **26**, 498 578

Yohimbine antagonism of the vasodepression elicited by organophosphates applied on ventral medulla oblongata

H. Edery [1] and H.A. Berman [2]

[1] *Israel Institute for Biological Research, Sackler School of Medicine,*
Tel-Aviv University, Ness-Ziona (Israel) and
[2] *Departments of Biochemistry and Pharmacology, School of Pharmacy,*
State University New York at Buffalo, Buffalo, NY (U.S.A.)

Abstract

The rostral ventral surface of medulla oblongata (RVMO) has been shown to constitute a selective target for organophosphate (op) cholinesterase inhibitors. The action of soman (S) as compared with (7-nitrobenz-2-oxa-1,3 diazole)aminopentyl methylphosphonofluoridate (NBD-AP-MPF), a fluorescent organophosphate has now been examined in anaesthetized cats pretreated with atropine sulphate. Blood pressure (BP), electrocardiogram (ECG) and respiration (R) were recorded. In some animals a cannula was implanted into the right lateral ventricle. Chemicals were bilaterally applied on RVMO by means of a perspex cannula and removed after 5 min. The application of 2.5 μg S or 60 μg NBD-AP-MPF elicited severe fall of BP which recovered only after 2 h in the case of the former and up to 45 min in the latter. Smaller doses produced corresponding responses of lesser magnitude. Accompanying R changes consisted in most cases of increased rate and reduced amplitude whereas in others the opposite or mixed alterations occurred. Frequently, sigh-like movements intermingled at periodic intervals with regular R deflections. The sighs were interpreted as aiming to correct blood gases balance. After application of

Correspondence: H. Edery, Israel Institute for Biological Research, Sackler School of Medicine, Tel-Aviv University, Ness-Ziona, Israel.

atropine on RVMO—but not by systemic administration—BP and R were restored whereas single repeated i.v. injection of 1 μg/kg noradrenaline produced only transient reversals without influencing the course of long lasting vasodepression. In contrast, the intraventricular administration of 250–500 μg yohimbine considerably reduced both the magnitude and extent of the vasodepression elicited by topically applied organophosphates. It is postulated that central α_2-adrenoceptors in contrast to vascular sites are likely involved in the op-induced vasodepression. The present work provides an indication that effective antagonists might be developed considering blockade of these receptors.

Introduction

The rostral ventral medulla oblongata (RVMO) has been shown to constitute a selective target site for cholinomimetic drugs [9] particularly organophosphate inhibitors of cholinesterases and their antagonists [7,8]. For instance, minute amounts of these toxicants applied on rostral ventromedullary sites—corresponding to the so called chemosensitive areas [18,23]—elicited prolonged vasodepression and respiratory disturbances. These centrally, in contrast to peripherally, elicited disturbances remained conspicuously resistant to systemic administration of cholinolytics and cholinesterase reactivators. Contrastingly, when these antagonists were topically applied on the ventromedullary sites, disturbances were not only reversed but the experimental animals could tolerate even continued infusion of large amounts of anticholinesterase without detrimental effects on blood pressure or respiration [7].

The purpose of the present work was to examine the central action of soman as compared with (7-nitrobenz-2-oxa-1,3 diazole)aminopentyl methylphosphonofluoridate (NBD-AP-MPF), a recently synthetized [1] fluorescent organophosphate. In addition, the hypothesis of possible involvement of central α_2-adrenoceptors in the long lasting vasodepression elicited by the organophosphates was considered.

Materials and Methods

Cats of both sexes (2500–3990 kg b.w.) anaesthetized with 25 mg/kg sodium pentobarbitone i.v. were used. Additional doses (5 mg/kg) of the anaesthetic were administered throughout the experiments in order to secure adequate surgical anaesthesia. This was ascertained by periodically checking absence of pedal reflex. Blood pressure (BP, pulsatile or mean) was recorded from left femoral artery by means of a pressure transducer; electrocardiogram (ECG, lead II) was also recorded. To perform i.v. injections a polythene tube was inserted in left femoral vein. Respiration was registered by means of a thermistor probe placed into a side arm of a plastic cannula tied to the trachea.

The ventral surface of medulla oblongata was exposed and a perspex applicator [10] was applied on its rostral sites (RVMO). The correct position was checked at the

end of experiments by colouring the areas with brom-phenol solution [8]. Solutions of chemicals (10 μl) were applied bilaterally and removed after 5 min by repeated washing with mock cerebrospinal fluid. In a series of 6 cats, preceding the fixation of applicator on ventral medulla, an indwelling Collison cannula was implanted in the right lateral ventricle. To perform intracerebroventricular (i.c.v.) injections, the ventral medulla applicator was temporarily removed and the animal placed up-right. The maximum volume injected was 0.25 ml and about 2 min afterwards the cat was returned to supine posture and the ventral medulla applicator replaced. Additional experimental details were described previously [7]. To block muscarinic cholinergic stimulation, 0.5 mg/kg· atropine sulphate was injected i.v. together with the first dose of aneasthetic and 1.5 mg/kg shortly before application of the anti-cholinesterases. Drug effects described in this paper were replicated in at least 3 separate animals and for comparative purposes some results which will be reported in extenso separately were also included.

The materials used included: sodium pentobarbitone (Abbott), atropine sulphate (Merck), nor-adrenaline (Sigma), yohimbine HCl (Plantex) as well as two organophosphate anticholinesterases, namely soman (S;pinacoly-methylphosphono-fluoridate) and the fluorescent compound NBD-AP-MPF (7-nitrobenz-2-oxa-1,3 diazole)aminopentyl methylphosphonofluoridate) [1]. Chemicals destined for application on the RVMO were dissolved in mock cerebrospinal fluid but the water-insoluble NBD-AP-MPF was dissolved in a mixture of 50% each propylene glycol and dimethylsulfoxide. Control experiments showed that the mixture was inert when applied on RVMO. Saline was the diluent for materials injected i.v.

Results

Effects on blood pressure

The bilateral application of S or NBD-AP-MPF on RVMO elicited a dose-related fall of BP whereas ECG changes were absent or very transient. The minimal dose producing hypotension was 0.5 μg in the case of S whereas NBD-AP-MPF was ineffective at 2.5 μg and a distinguishable fall occurred only after application of 5 μg. In Fig. 1 the log doses were plotted against mean BP fall. It may be seen that the slope for S was rather steep in contrast with the one for NBD-AP-MPF. After removal of the anticholinesterases, BP was eventually restored completely in most cases, and in others it stabilized at a level slightly lower than the initial one. Times for full recovery after application of the largest doses were 2 h to 3 h 25 min in the case of 2.5 μg S and 35–45 min after 60 μg NBD-AP-MPF. On the other hand, unilateral application of these doses was ineffective.

Effects on respiration

Whereas hypotension was a constant feature caused by bilateral application of the anticholinesterases, the accompanying respiratory changes varied. In most cases respiratory rate increased and amplitude decreased, but in others the opposite or mixed changes occurred. In the majority of the experiments sigh-like movements
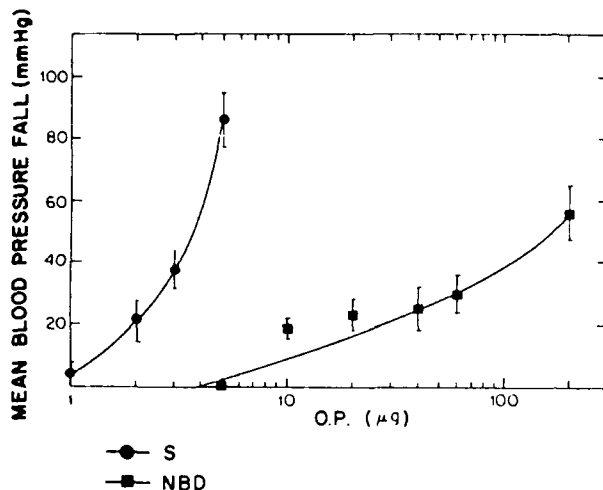
Fig. 1. Diagram showing mean blood pressure fall (mm Hg) elicited by bilateral application on rostral ventral medulla oblongata of organophosphates (O.P.): S, soman; NBD, NBD-AP-MPF. Doses (μg) in logarithmic scale.

intermingled at regular intervals with ordinary respiratory movements as shown in Figs. 2–4. Respiration usually normalized simultaneously or independently of BP but in some experiments remained accelerated and at reduced amplitude despite of BP having been totally restored.

Antagonism by atropine, noradrenaline or yohimbine

Bilateral application of 500 μg atropine sulphate performed at the peak effects induced by S [29] or NBD-AP-MPF, restored BP and regularized respiration. Fig. 2 illustrates some of these findings.

In 3 cats, bolus injection of 1 μg/kg noradrenaline was administered i.v. at various intervals (up to 4 times) during the course of vasodepression provoked by bilateral application of 2.5 μg S. As shown in Fig. 3, immediately after each single injection of noradrenaline there was a transient BP rise. However, in no experiment was the typically long time-course of hypotension induced by S appreciably shortened after repeated administrations of noradrenaline.

The hypothesis of possible involvement of central α_2-adrenoceptors [16] in the vasodepression provoked by organophosphates was then considered and it seemed appropriate to test yohimbine as potential antagonist. In a series of experiments (6 cats) a hypotensive response after bilateral application of 30 μg NBD-AP-MPF was first obtained. When BP had regained its initial level, 250 or 500 μg yohimbine was injected i.c.v. Regardless the dose, yohimbine elicited a short lived BP fall followed by a progressive rise until BP became stabilized at (a) a level slightly higher than the initial one (4 cats) or (b) declined eventually to normal (2 cats). When BP was steady, the application of NBD-AP-MPF was repeated in all 6 cats. In case (a) the application of NBD-AP-MPF brought BP down only to its normal level whereas in
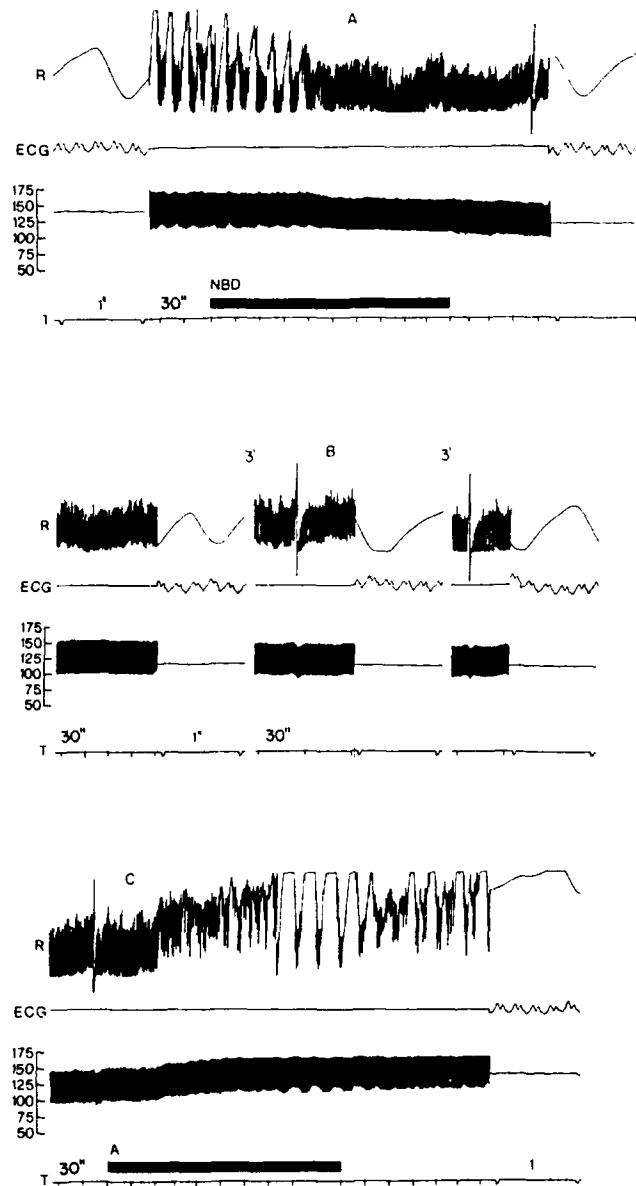
Fig. 2. Cat, female, 3.990 kg b.wt., anaesthetized with sodium pentobarbitone and pretreated with atropine sulphate. Record of respiration, R, electrocardiogram (ECG), blood pressure (pulsatile and mean, scale in mm Hg) and time (T, 1', 30"). Time gap between panel A-B 3 min, B-C 5 min. Upper numbers indicate time intervals. Horizontal bar denotes bilateral application on rostral ventral medulla oblongata (RVMO) of 30 µg NBD-AP-MPF (NBD) or 500 µg atropine sulphate (A).
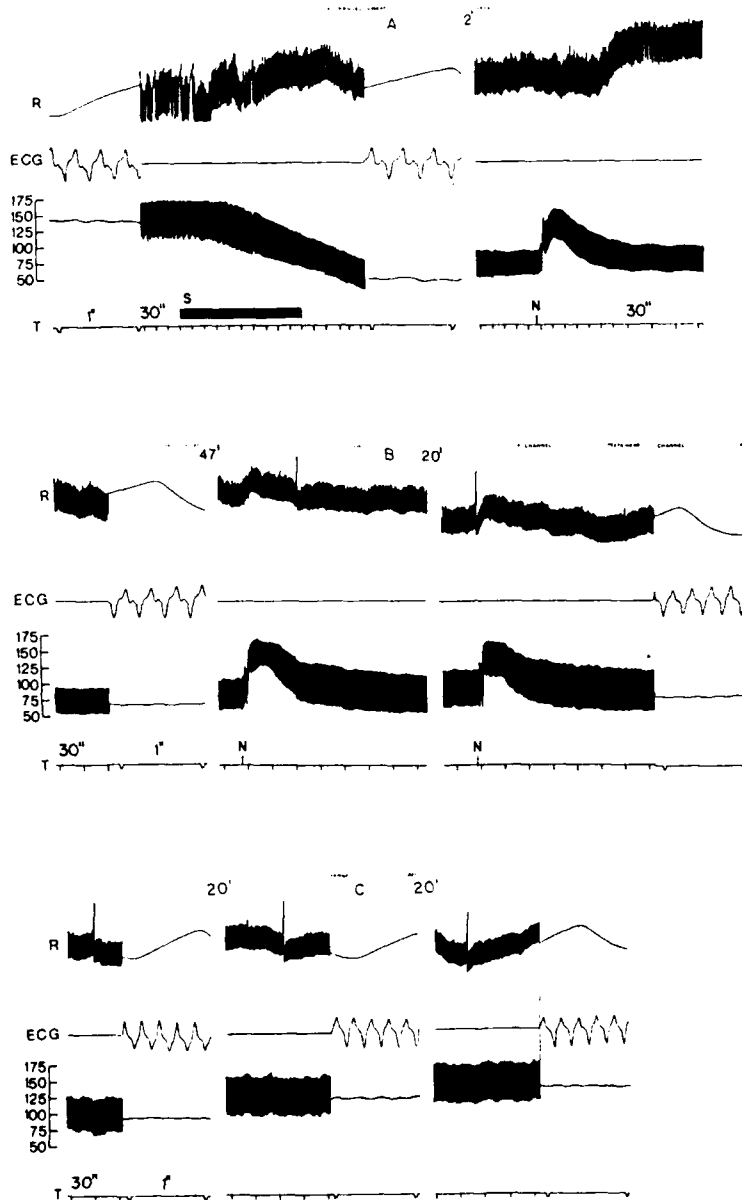
234

Fig. 3. Cat female 2.780 kg b.w. Conditions and abbreviations as in Fig. 2. Time gap between A–B 35 min. Horizontal bar denotes bilateral application on RVMO of 2.5 μg soman (S). Signal in time line indicates i.v. injection of 1 μg/kg noradrenaline (N).

case (b) the vasodepression was considerably reduced: fall being 12 and 15 mm Hg vs 28 and 34 mm Hg, respectively in control responses. Furthermore, in all above mentioned experiments, 2.5 μg S was applied bilaterally when BP had recovered
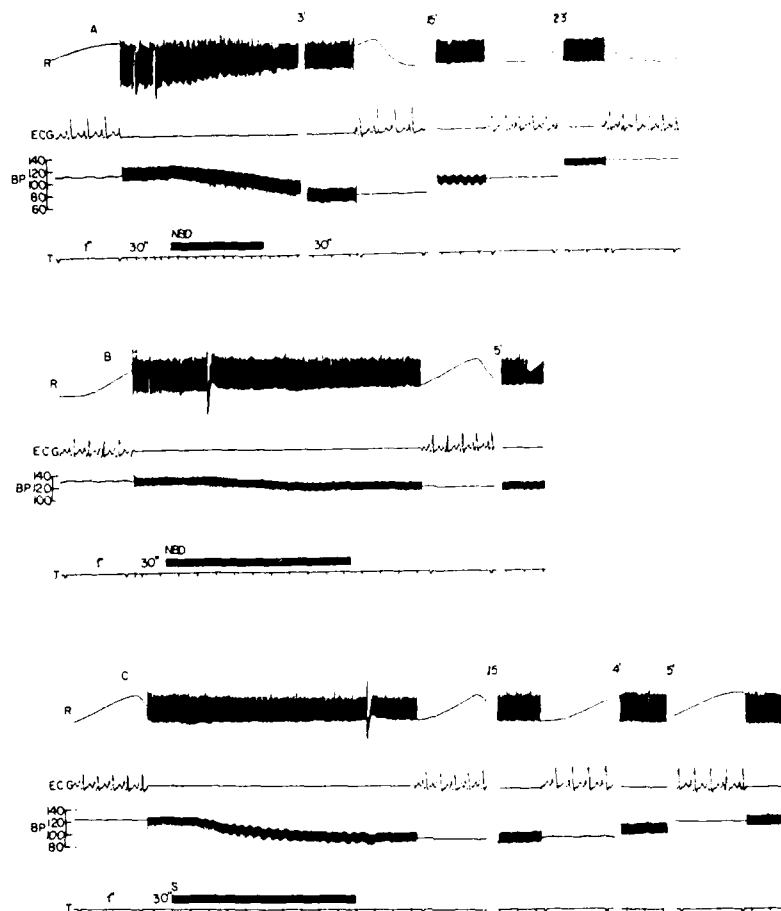
Fig. 4. Cat, female 2.500 kg b.w. Conditions and abbreviations as in Fig. 2. Between panel A and B 30 min elapsed during which 500 μg yohimbine was injected into the right lateral ventricle. Interval between B–C 5 min. Horizontal bar denotes bilateral application on RVMO of 30 μg NBD-AP-MPF(NBD) or 2.5 μg soman (S).

from the second application of NBD-AP-MPF. Under these circumstances S-induced vasodepression was not only of small magnitude, 35 ± 6 mm Hg compared with 86.50 ± 8.10 in control cats, but also of shorter duration, 20–35 min against 2 h to 3 h 15 min in corresponding experiments without yohimbine. Fig. 4 illustrates some of these findings. Moreover in all these experiments it was noted that after administration of yohimbine, the respiratory disturbances which accompanied the hypotension, were less severe.

To further explore the potential of yohimbine as antagonist, the drug was administered i.v. at the nadir of hypotension induced by S application to 6 other cats. In 2 out of 3 animals which received 0.5 mg/kg yohimbine i.v. after application

of 1.5 μg S, the BP was fully restored within 20 and 55 min of drug injection vs 1 h 10 min to 1 h 40 min in controls. However, in the third cat no clear beneficial effect was noted. In 3 other animals, namely A, B and C, S was applied at the highest dose examined i.e. 2.5 μg whereas the i.v. dose of yohimbine administered was 0.5 mg/kg to cat A and 0.25 mg/kg to cats B and C. In the two latter, BP was brought to initial level 25 min and 45 min after drug injection. Furthermore, shortly after BP had stabilized, a second application of S elicited in cat B a minor fall and no hypotension in cat C. Contrastingly in cat A, BP did not recover even after 2 h of yohimbine injection, and the animal was sacrificed after that time.

Discussion

A salient finding in this work was that yohimbine i.c.v. administered, effectively reversed or prevented the otherwise long lasting vasodepression elicited by organophosphates. Most probably yohimbine antagonism had been effected by restoration of previously diminished vascular tone. Reduction of this latter and concomitant decrease of peripheral resistance have been repeatedly postulated as the essential mechanism for the anticholinesterase-induced hypotension presenting conspicuous refractoriness to systemic administration of cholinolytics [5,7,8,22]. The normal vascular tone has been shown to be regulated through sympathetic outflow originating in hypothalamic neurons and other descending monoaminergic pathways [12,19,20,24]. In addition, pharmacological evidence suggested the presence of α_2-adrenoceptors regulating noradrenaline release, in central adrenergic neurons [2,13,16,25,27]. It could then be reasonably postulated that yohimbine reinstated the sympathetic vascular tone and consequently peripheral resistance by blockade of central α_2-adrenoceptors. We favour a central mechanism because yohimbine was consistently effective after i.c.v. whereas by i.v. injection antagonism was less evident or absent. The variation could be attributed to the fact that systemically administered yohimbine has been reported [11] to interact with central and peripheral vascular α_2-adrenoceptors [17] as well as other amine receptors (dopamine, serotonin). All these are capable of influencing the type and magnitude of blood pressure responses depending on the dose, number and sensitivity of receptors populating each particular vascular bed, degree of blockade, etc. These factors then, would make the resultant blood pressure response to i.v. yohimbine less predictable. The transient reversal of the hypotension produced by exogenous noradrenaline may be readily explained. Its pressor effect in the cat is effected by peripheral vasoconstriction [14] attributed to activation of vascular, in contrast to central, α_2-adrenoceptors [17]. To reinstate adequate peripheral resistance, it would probably be more adequate to administer the catecholamine not in single injections but in prolonged infusion as it has been shown to be successful in different experimental conditions [28].

The protean character of respiratory changes elicited by application of anticholinesterases in the present work was consistent with similar previous observations [7,8]. The variability strongly supports the concept [15] of functional independence

of respiratory and vasodepressor responses elicited from ventral medulla which were probably also mediated by different neural networks [23]. The sigh-like movements, which frequently interrupted normal respiratory deflections, have also been observed in acute hypotension and neurocirculatory asthenia in humans and were supposed to correct deficient PO_2-PCO_2 balance [3,4]. The current opinion holds that sigh is reflexly generated in hypoventilated lung patches and the deep inspiration phase aims to re-expand discrete areas of atelectasis [3,21]. It could then be speculated that the increased cholinergic activity resulting from cholinesterase inhibition [6,7] in superficial RVMO cells could have induced vasodepression along with broncho-constriction. Thus, the possibility arises that these cells might have some involvement in bronchomotor control in addition to their role in generation of respiratory drive [23].

The antagonism by topically applied atropine of NBD-AP-MPF and S was according to expectations. It has already been shown that a number of topically applied cholinolytic agents, probably acting on cholinergic receptors of RVMO [6,7] effectively reversed vasodepressor and respiratory disturbances induced by a number of anticholinesterases, either topically [8] or i.v. administered [7]. On the other hand the question arises concerning the ineffectiveness of systemically administered atropine. The reason could be that by the latter route, insufficient concentration of the drug was attained on a critical central site such as the superficial cells of RVMO. NBD-AP-MPF was considerably less potent than S as far as induction of vaso-depression and ventilation disturbances were concerned. The reason could be lesser intrinsic anticholinesterase activity [1] and/or inherent poor diffusibility owing to the NBD-AP-MPF bulky molecule.

Hitherto, the rationale behind the search for antagonists against organophosphate anticholinesterases has implied mainly cholinergic mechanisms. A number of cholinolytics and cholinesterases reactivators have been reported to reverse most of the deleterious effects [26]. However it has been shown in cats [7] that central vasodepression remains an exception, unless antagonists were deposited directly on RVMO. As corollary, the present work seems to provide an indication that central hypotension may also be overcome through proper manipulation of central α_2-adrenoceptors.

Acknowledgement

References

1 Berman, A.H., Olshefski, D.F., Gilbert, M. and Decker, M.M., Fluorescent phosphonate labels for serine hydrolases, J. Biol. Chem., 260 (1985) 3462–3468.

2 Bousquet, P., Rouot, B. and Schwartz, J., The central α-adrenoceptors: some new aspects, Trends Pharmacol. Sci., 4 (1983) 206–208.

3 Comroe, J.H., Physiology of Respiration, Yearbook Medical Publishers Incorporated Chicago, London, 1977, 232 pp.

4 Churchill-Davidson, H.C., A Practice of Anaesthesia, Lloyd-Luke (Medical Books) Ltd., London, 1979, 96 pp.

5 De Neef, J.H., Borgdorff, P. and Porsius, A.J., Inhibition of efferent sympathetic nerve activity by centrally administered paraoxon in the cat, Eur. J. Pharmacol., 81 (1982) 123–127.

6 Dermietzel, R., Willenberg, I. and Leibstein, A., Histochemical studies on the central chemosensitive fields of the medulla oblongata. In M.E. Schlaefke, H.P. Koepchen and W.R. See (Eds.), Central Neurone Environment and the Control Systems of Breathing and Circulation, Springer, Berlin, Heidelberg, New York, 1983, pp. 251–256.

7 Edery, H., Target sites for anticholinesterases, cholinolytics and oximes on ventral medulla oblongata. In M.E. Schlaefke, H.P. Koepchen and W.R. See (Eds.), Central Neuron Environment and the Control Systems of Breathing and Circulation, Springer, Berlin, Heidelberg, New York, 1983, pp. 238–250.

8 Edery, H. and Guertzenstein, P.G., A central vasodepressor effect of dyflos, Br. J. Pharmacol., 50 (1974) 481–487.

9 Feldberg, W., The ventral surface of the brain stem: a scarcely explored region of pharmacological sensitivity, Neuroscience, 1 (1976) 427–441.

10 Feldberg, W. and Guertzenstein, P.G., A vasodepressor effect of pentobarbitone sodium, J. Physiol. (London), 244 (1972) 83–103.

11 Goldberg, M.R. and Robertson, D., Yohimbine: a pharmacological probe for study of the α-adrenoceptor, Pharmacol. Rev., 35 (1983) 143–480.

12 Hilton, S.M. and Spyer, K.M., Central nervous regulation of vascular resistance, Ann. Rev. Physiol., 42 (1980) 399–411.

13 Issac, L., Clonidine in the central nervous system: site and mechanism of hypotensive action, J. Cardiovasc. Pharmacol., 2 (1980) S5–S19.

14 Karim, S.M., The mechanism of the pressor action of noradrenaline in pithed cats, Br. J. Pharmacol., 27 (1966) 17–32.

15 Koepchen, H.P., Respiratory and cardiovascular "centres": functional entity or separate structures? In M.E. Schlaefke, H.P. Koepchen and W.R. See (Eds.), Central Neurone Environment and the Control Systems of Breathing and Circulation, Springer, Berlin, Heidelberg, New York, 1983, pp. 221–237.

16 Langer, S., Synaptic regulation of the release of catecholamines, Pharmacol. Rev., 32 (1981) 337–362.

17 Langer, S.Z. and Shepperson, N.B., Recent developments in vascular smooth muscle pharmacology: the post synaptic α-2 adrenoceptor, Trends Pharmacol. Sci., 3 (1982) 440–443.

18 Loeschcke, H.H., Central chemosensitivity and the reaction theory, J. Physiol. (London), 332 (1982) 1–24.

19 Loewy, A.D., Descending pathways to the sympathetic preganglionic neurons. In H.G.J.M. Kuypers and G.F. Martin (Eds.), Descending Pathways to the Spinal Cord. Progress in Brain Research, Vol. 57, Elsevier, Amsterdam, 1982, pp. 267–277.

20 Loewy, A.D. and Neil, J.J., The role of descending monoaminergic systems in central control of blood pressure, Fed. Proc., 40 (1981) 2778–2785.

21 Nunn, J.F., Applied Respiratory Physiology, Butterworths, London, 1978, 54 pp.

22 Preston, E. and Heath, C., Atropine-insensitive vasodilatation and hypotension in the organophosphate-poisoned rabbit, Arch. Int. Pharmacodyn. Ther., 200 (1972) 231–244.

23 Schlaefke, M.E., Central chemosensitivity: a respiratory drive, Rev. Physiol. Biochem. Pharmacol., 90 (1981) 172–244.

24 Spyer, K.M., Central nervous integration of cardiovascular control, J. Exp. Biol., 100 (1982) 109–128.

25 Starke, K., Presynaptic receptors, Ann. Rev. Pharmacol. Toxicol., 21 (1981) 7–30.

26 Taylor, P., Anticholinesterases agents. In L.S. Goodman and A. Gilman (Eds.), The Pharmacological Basis of Therapeutics, Macmillan, New-York, 1980, pp. 100–119.

27 Timmermans, P.B.W.M. and Zwieten, P.A., α-2 Adrenoceptors: classification, localization, mechanisms and targets for drugs, J. Med. Chem., 25 (1982) 1390–1401.

28 Vanhoutte, P.M., Introductory remarks: alpha- and beta-adrenergic receptors and the cardiovascular system, J. Cardiovasc. Pharmacol., 3 (1981) S1–S13.

29 Wei, N. and Tian, W., Effects of artificial respiration, maintaining blood pressure and atropine on soman-induced respiratory depression in rabbits, Acta Pharmacol., Sin., 2 (1981) 170–175.

Fluorescent Phosphonate Labels for Serine Hydrolases

KINETIC AND SPECTROSCOPIC PROPERTIES OF (7-NITROBENZ-2-OXA-1,3-DIAZOLE)AMINOALKYL METHYLPHOSPHONOFLUORIDATES AND THEIR CONJUGATES WITH ACETYLCHOLINESTERASE MOLECULAR FORMS*

Harvey Alan Berman‡, Dennis F. Olshefski, Mark Gilbert, and M. M. Decker

From the Department of Biochemical Pharmacology, State University of New York at Buffalo, Buffalo, New York 14260

The synthesis, kinetic, and spectral characterization of (7-nitrobenz-2-oxa-1,3-diazole)aminoethyl and (7-nitrobenz-2-oxa-1,3-diazole)aminopentyl methylphosphonofluoridate are described. These homologous organophosphorous agents contain the environmentally sensitive 7-nitrobenz-2-oxa-1,3-diazole chromophore. They inhibit acetylcholinesterase from *Torpedo* at rates exceeding 10^7 M^{-1} min^{-1} to form long-lived conjugates with one chromophore/80-kilodalton subunit. The intensity, position, and line width of the absorption spectra of the conjugates and reactivation kinetics in the presence and absence of the bisquaternary oxime 1,1'-trimethylene-bis(4-formylpyridinium bromide) dioxime indicate that these agents form conjugates in which the NBD-aminoalkyl moieties experience distinctive microscopic environments within the active center.

NBD-aminoethyl methylphosphono-acetylcholinesterase undergoes oxime-induced as well as spontaneous reactivation at rates that are 3.6 and 35 times faster, respectively, than the corresponding rates measured for the NBD-aminopentyl conjugate. Hence, reactivation exhibits a marked dependence on structure of the methylphosphonate.

Fluorescence emission at wavelengths greater than 520 nm is highly quenched and exhibits quantum efficiencies of less than 5%. Absorption maxima for the covalent NBD-aminoethyl methylphosphono-acetylcholinesterase appear at 475–480 nm while those for the corresponding NBD-aminopentyl methylphosphono-acetylcholinesterase appear at 485–490 nm. Bandwidths of the absorption maxima are substantially broader for the acetylcholinesterase adduct with NBD-aminoethyl methylphosphonofluoridate (3870 cm^{-1}) than for the enzyme adduct with NBD-aminopentyl methylphosphonofluoridate (2870 cm^{-1}). The CD spectrum of NBD-aminopentyl methylphosphono-acetylcholinesterase shows optical activity coincident with the shape and position of the absorption spectrum. In contrast, in addition to optically active transitions at the absorption maxima, the CD spectrum of NBD-aminoethyl methylphosphono-acetylcholinesterase shows intense optical activity at 430 nm, a wavelength region coincident with the region of spectral broadening.

The spectral properties of α-chymotrypsin conjugates formed by reaction with the two probes are different, and the respective spectra differ also from those observed for the acetylcholinesterase conjugates. These results indicate that there is a reciprocal relationship between the structure of the probe and the structure of the active center. Absorption spectra obtained for conjugates with the 5.6 S hydrophobic dimeric form of acetylcholinesterase from *Torpedo*, which has an amino acid composition that is unique from the 11 S tetrameric form, are essentially equivalent with that of the 11 S form, providing evidence independent of sequence analysis for a homology within the active centers of these two genetically distinct enzymes.

Site-specific fluorescent probes have been useful in delineating equilibrium and kinetic features of ligand association with acetylcholinesterase and have been employed to assess microscopic topography of the enzyme surface (1–4). Probes specific for the active center, in particular, allow one to exploit the presence within the catalytic cavity of a nucleophilic serine that reacts with organophosphorous agents to form long-lived enzyme intermediates suitable for spectroscopic study (5–7). The availability of fluorescent organophosphonates characterized by a common homologous structure would prove advantageous in assessing both the protein environment and the spatial dimensions of the active center. Aminoalkyl conjugates of 4-chloro-7-nitrobenz-2-oxa-1,3-diazole (NBD-Cl¹), in particular, when examined in solvents of different polarity undergo dramatic changes in their absorption and fluorescence spectra and, hence, are expected to serve as sensitive probes of the protein environment within the catalytic center (8).

This paper reports the synthesis, kinetics of inhibition and reactivation, and absorption, fluorescence and circular dichroism spectra of a homologous pair of methylphosphonofluoridates containing aminoalkyl conjugates of NBD-Cl. The new probes are designated NBD-aminoethyl and NBD-aminopentyl methylphosphonofluoridate, NBD-AE-MPF and NBD-AP-MPF, respectively, and by virtue of the different chain lengths separating the fluorophore from the reactive methylphosphonyl group, their spectroscopic characteristics serve to report on the protein environment within different regions of the active center.

¹ The abbreviations used are: NBD-Cl, 4-chloro-7-nitrobenz-2-oxa-1,3-diazole; NBD, 7-nitrobenz-2-oxa-1,3-diazole; NBD-AE-MPF, NBD-aminoethyl methylphosphonofluoridate; NBD-AP-MPF, NBD-aminopentyl methylphosphonofluoridate; TMB-4, 1,1'-trimethylenebis(4-formylpyridinium bromide) dioxime; AchE, acetylcholinesterase.

These probes are employed to examine acetylcholinesterase from *Torpedo californica*. When isolated by tryptic digestion of *Torpedo* electroplax, the enzyme exists as a tetrameric species exhibiting a sedimentation coefficient of 11 S (9). Low salt extraction in the absence of tryptic digestion affords, in contrast, a dimeric species characterized by a sedimentation coefficient of 5.6 S (10, 11). Both NBD-AE-MPF and NBD-AP-MPF are found to be potent and specific inhibitors of the 11 S "lytic" form of acetylcholinesterase and form conjugates with a stoichiometry of one methylphosphonyl moiety/subunit. The spectral characteristics of these homologous probes conjugated with the different molecular forms of acetylcholinesterase are presented and compared with those determined for the corresponding conjugates with α-chymotrypsin.

EXPERIMENTAL PROCEDURES

Materials—α-Chymotrypsin (Type 1 S) and TMB-4 were products of Sigma. The 11 S or lytic form of acetylcholinesterase from *T. californica* was purified to homogeneity by affinity chromatography of electroplax homogenates subjected to mild tryptic digestion (9). The dimeric low salt soluble form was isolated from the first supernatant fraction of electroplax homogenates by affinity chromatography as described by Lee *et al.* (11).

The fluorescent conjugates were formed by reaction of purified enzyme with a 1.5–3-fold excess of the methylphosphonofluoridate delivered from a concentrated stock solution in acetonitrile. In a typical preparation, the enzyme was present in concentrations greater than 2×10^{-6} M in subunit sites. The reaction mixture was passed through a Sephadex G-25 column at 4 °C. Labeled enzyme appeared in the void volume and was collected and dialyzed extensively against buffer. The buffer medium was a 0.01 N Tris-Cl buffer, pH 8.0, containing 0.1 N NaCl and 0.04 M MgCl₂.

Acetylcholinesterase activity was measured by titration in a Radiometer TTT-60 pH-stat titrator. NMR spectra were obtained on Varian T-60 and EM-390 spectrometers with tetramethylsilane as an internal standard; proton signals are reported in parts per million (δ). Ultraviolet spectra were obtained on a Cary 210 or a Beckman UV-25 spectrometer. Fluorescence spectra were obtained on an Aminco-Bowman Ratio II spectrometer equipped with a thermostatted cell compartment and a Hamamatsu R-928P photomultiplier tube.

Circular dichroism of the conjugates was examined on a JASCO J41C spectropolarimeter operating at 25 °C. Optical activity is reported as molar ellipticity $[\theta]_\lambda$ (degrees-cm²/decimole) which is calculated according to Equation 1 from the observed ellipticity, θ_{obs} (degrees), and the molecular weight of the chromophore, where d and c denote, respectively, the path length (centimeters) and the chromophore concentration (grams/milliliter) (12). For conjugates formed from both probes,

$$[\theta]_\lambda = \frac{\theta_{obs} \times M_r}{c \times d \times 10} \tag{1}$$

a M_r of 207.17, representing the NBD-aminoethyl moiety, was employed. The path length was 1 cm.

Elemental analyses were performed at Galbraith Laboratories, Inc., Knoxville, TN, and are within ±0.4% for each element analyzed. The purity of compounds was assessed by thin layer chromatography on silica gel plates (Eastman Chromagram); products were detected by UV fluorescence. Column chromatography was carried out with silicic acid. Melting points were determined on a Mel-Temp apparatus and are uncorrected.

Inhibition and Subsequent Reactivation of Acetylcholinesterase—Kinetics of inhibition of acetylcholinesterase by fluorescent methylphosphonates were monitored by the general procedure of Hart and O'Brien (13), with *p*-nitrophenyl acetate as substrate. The reaction medium was 0.1 M sodium phosphate, pH 7.0.

Reactivation of the phosphonylated enzyme in the presence and absence of TMB-4 (1 mM) was carried out at 25 °C in 0.01 N Tris-Cl buffer, pH 8.0, containing 0.1 N NaCl and 0.04 M MgCl₂. The enzyme for these studies was passed through a Sephadex G-25 column and dialyzed overnight against buffer. Reactivation studies were based on return of catalytic activity against 0.5 mM acetylcholine chloride following 200–3000-fold dilution of the enzyme prior to assay. To monitor enzyme stability over long intervals, native enzyme was incubated and examined under equivalent conditions.

Synthesis of Fluorescent Methylphosphonates—Methylphosphonodichloridate was synthesized by reaction of methyl dimethylphosphonate with PCl₅ (15) and was converted to methylphosphonodifluoridate by treatment with NaF in tetramethylene sulfone (16, 17), as previously described (5).

1a $n = 2$
1b $n = 5$

2a $n = 2$
2b $n = 5$
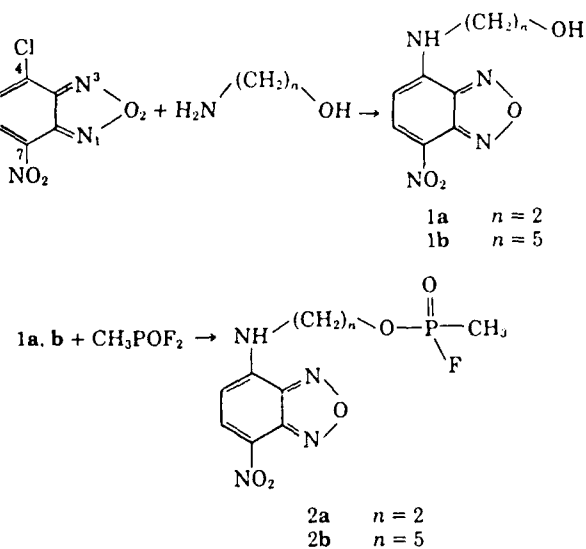
SCHEME 1

Scheme 1 illustrates the synthesis of the fluorescent alcohols and methylphosphonofluoridates. NBD-Cl was reacted with either 2-aminoethanol or 5-amino-1-pentanol to afford NBD-aminoethanol (1a) and NBD-aminopentanol (1b), respectively. Reaction of these alcohols with methylphosphonodifluoridate afforded the corresponding methylphosphonofluoridates (2a and b). The course of the reaction is readily followed by monitoring the NMR spectral changes of the methyl group. The difluoridate exhibits a first-order spectrum consisting of a doublet of triplets that collapse to a doublet of doublets upon formation of the monofluoridate (5).

NBD-aminopentanol (1b)—To a solution of NBD-Cl (3.8 g, 0.019 mol) in methanol was added dropwise a solution of aminopentanol (8.15 g, 0.079 mol) in methanol. The reaction was allowed to proceed under reflux, and the reaction progress was followed by monitoring changes in thin layer chromatography. After 3 h, the reaction mixture was allowed to cool to room temperature, reduced *in vacuo* to an oil, and purified by chromatography on silicic acid with mixtures of chloroform and hexane. Crystallization from CHCl₃ afforded yellow needles (3.09 g, 62–78% yield), m.p. 97.5–98.5 °C. NMR (CDCl₃) 8.45 (d, $J = 8$ Hz, 1H, NBD), 6.13 (d, $J = 8$ Hz, 1H, NBD), 3.66 (t, $J = 6$ Hz, 2H, α-methylene), 3.4 (t, $J = 6$ Hz, ε-methylene), 1.68 (m, 6H, β,γ,δ-methylenes).

Calculated: C 49.62 H 5.26 N 21.03 O 24.06
Found: C 49.62 H 5.37 N 21.00 O 23.93

λ_{max} (H₂O) = 480 nm; $\epsilon_{H_2O} = 2.8 \pm 0.1 \times 10^4$ M⁻¹ cm⁻¹.

NBD-aminoethanol (1a)—This material was prepared by a procedure similar to that for NBD-aminopentanol or was purchased from Molecular Probes. The melting points of the final product (m.p. 144.5–145.5 °C) and purchased material (144–145 °C) were comparable. λ_{max} (H₂O) = 475 nm; $\epsilon_{H_2O} = 2.5 \pm 0.1 \times 10^4$ M⁻¹ cm⁻¹.

NBD-aminopentyl Methylphosphonofluoridate (2b)—To a solution of CH₃POF₂ (2.311 g, 0.0231 mol) in CH₂Cl₂ in a 3-necked round bottom flask equipped with a reflux condenser, CaCl₂ drying tube, and a pressure equalizing dropping funnel was added a solution of NBD-aminopentanol (1.5 g, 0.0056 mol) and triethylamine (0.68 g, 0.0067 mol) in CH₂Cl₂. The reaction was allowed to proceed under reflux for 6 h, allowed to cool to room temperature, diluted with CH₂Cl₂, and washed two times with saline. The organic layer was dried over Na₂SO₄, filtered, reduced *in vacuo*, and purified by passage through a column of silicic acid. Crystallization from mixtures of CHCl₃ and ether afforded orange crystals (1.0 g, 50% yield), m.p. 115.5–116.5 °C. NMR (CDCl₃) 8.45 (d, $J = 8$ Hz, 1H, NBD), 6.15 (d, $J = 8$ Hz, 1H, NBD), 7.1 (relaxed t, $J = 6$ Hz, NH), 4.29 (m, 2H, α-methylene) 3.56 (q, $J = 6$ Hz, 2H, ε-methylene), 1.65 (dd, $J_{HF} = 6$

Hz, J_{HP} = 18 Hz, 3H, methyl), 1.8 (m, 6H, δ,γ,δ-methylene).

Calculated: C 41.6 H 4.6 N 16.18 P 8.96 F 5.49
Found: C 41.49 H 4.64 N 16.04 P 8.85 F 5.33

NBD-aminoethyl Methylphosphonofluoridate (2a)— This material was synthesized as described above for the aminopentyl derivative. Crystallization of the product isolated after chromatography from silicic acid afforded yellow-orange crystals, m.p. 154.5–155 °C. NMR (dimethyl sulfoxide-d_6) 8.5 (d, J = 8 Hz, 1H, NBD), 6.4 (d, J = 8 Hz, 1H, NBD), 4.35 (m, 2H, α-methylene), 3.8 (t, J = 5 Hz, 2H, β-methylene), 1.7 (dd, J_{HF} = 6 Hz, J_{HP} = 18 Hz, 3H, methyl).

Calculated: C 35.54 H 3.31 N 18.42 P 10.18 F 6.25
Found: C 35.46 H 3.36 N 18.21 P 10.3 F 6.01

RESULTS

Inhibition of Acetylcholinesterase by Fluorescent Methylphosphonates— Inhibition of acetylcholinesterase by the fluorescent methylphosphonates proceeded rapidly and could be measured by conventional techniques only at submicromolar concentrations of inhibitor. The bimolecular reaction constants exceeded values of 10^7 M^{-1} min^{-1} (Table I) and were 200–1000-fold greater than those for the lipid-soluble phosphates paraoxon, diisopropylphosphorofluoridate, and maloxon (13, 14, 18). When inhibitor was in excess, the observed first-order kinetics were indicative of a single phosphonylating species reacting with a homogeneous class of independent sites.

NBD-AP-MPF was stable to hydrolysis in buffer, and its inhibition of acetylcholinesterase was measured readily. NBD-AE-MPF, in contrast, was hydrolyzed at a measurable rate. Thus, the rate of loss of enzyme inhibition declined following incubation of inhibitor for different times prior to reaction with enzyme. Ashani *et al.* (19) have described a method for determining inhibition constants of labile agents that concomitantly undergo rapid spontaneous hydrolysis. Using this method, we obtained an inhibition constant of 2.4 × 10^7 M^{-1} min^{-1}, a value comparable to that obtained for NBD-AP-MPF, and a value of 1.7 ± 0.4 min^{-1} for the alkaline hydrolysis rate constant.

Reactivation of the Methylphosphonyl-acetylcholinesterase Conjugates— Reactivation at 25 °C in the presence of the bisquaternary bisoxime nucleophile TMB-4 (1 mM) as well as spontaneous reactivation in its absence behaved as first-order processes to greater than 90% completion (Fig. 1 and Table

TABLE I

Inhibition of acetylcholinesterase and subsequent reactivation parameters on methylphosphonyl-AchE

K_i, k_r, and k_s denote the bimolecular reaction constant, oxime-induced, and spontaneous reactivation rate constants, respectively.

	K_i[a]	k_r[b]	k_s[b]	k_r/k_s
	$M^{-1} min^{-1}$	h^{-1}	h^{-1}	
NBD-AP-MPF	(5.4 ± 2.3) × 10^7	0.03 ± 0.01	2.3 ± 1.3 × 10^{-4}	130
NBD-AE-MPF	(2.0 ± 0.4) × 10^7	0.11 ± 0.02	8.2 ± 2.5 × 10^{-3}	13

[a] Inhibition constants were determined by the general procedure of Hart and O'Brien (13). The fluorescent methylphosphonates and *p*-nitrophenylacetate (1 mM) were added to a cuvette containing 0.1 M sodium phosphate buffer, pH 7.0. After positioning the cuvette in the light path of the spectrophotometer, acetylcholinesterase was added to give an estimated concentration of 1 × 10^{-8} M in active sites, and the reaction was measured by the increase in optical density at 402 nM.

[b] Reactivation rates were obtained by incubation of the enzyme conjugate at 25 °C in the absence or presence of TMB-4 (1 mM). The catalytic activity of aliquots, taken at different times, was measured against 0.5 mM acetylcholine after a 200–1000-fold dilution of enzyme from the incubation medium.

[c] Determined by employing the method of residual activity (18). The hydrolysis rate was determined to be 1.7 ± 0.4 min^{-1}.
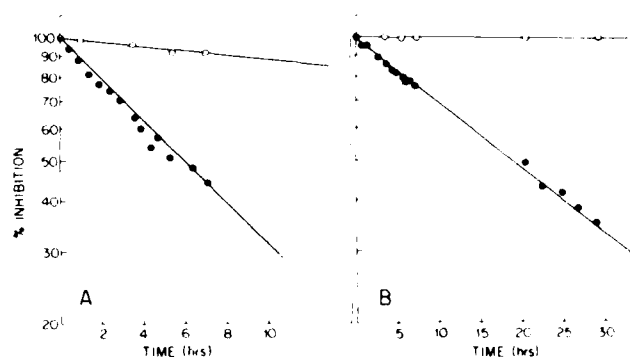

FIG. 1. **Reactivation kinetics of NBD-aminoalkyl methylphosphono-acetylcholinesterase conjugates in the presence and absence of TMB-4.** NBD-aminoalkyl methylphosphonyl-acetylcholinesterase forms were present at concentrations of 2–4 × 10^{-6} M in subunit sites in a 0.01 N Tris-Cl buffer, pH 8.0, containing 0.1 N NaCl and 0.04 M MgCl$_2$. Reactivation was conducted in the presence (● ●) and absence (○ ○) of TMB-4 (0.001 M). *A* presents results obtained for reactivation of NBD-aminoethyl methylphosphono-acetylcholinesterase. In the presence of oxime reactivation proceeds with a rate constant of 0.11 ± 0.02 h^{-1}, while in the absence of oxime the reactivation rate constant of 8.2 ± 2.5 × 10^{-3} h^{-1} is substantially slower. *B* presents results obtained for reactivation of NBD-aminopentyl methylphosphono-AchE for which the corresponding reactivation rate constants are calculated to be 0.03 ± 0.01 h^{-1} and 2.3 ± 1.3 × 10^{-4} h^{-1}, respectively, in the presence and absence of oxime.

I). NBD-aminoethyl methylphosphono-AchE underwent spontaneous reactivation nearly 40 times more rapidly than the corresponding NBD-aminopentyl methylphosphono conjugate, whereas the respective oxime-induced rates differed by 3.6-fold.

Spectroscopic Characterization of the Enzyme Conjugates— Upon transfer of NBD-aminopentanol from solvents of low to high dielectric constant, the absorption spectrum (Fig. 2) underwent shifts in wavelength of nearly 40 nm concomitant with a doubling of the extinction coefficient and a broadening of the spectral bandwidth. The emission spectra exhibited comparable blue shifts. These results are indicative of behavior expected for dipolar molecules undergoing marked changes in the transition dipole moment upon absorption and emission of radiation. This behavior for a neutral NBD-containing moiety is similar to that reported for NBD-alanine (20).

Acetylcholinesterase conjugates with NBD-aminoethyl- and NBD-aminopentyl methylphosphonofluoridates exhibited distinct absorption spectra (Fig. 3 and Table II). The NBD-aminopentyl adduct with acetylcholinesterase had an absorption maximum at 485–490 nm whereas that for the NBD-aminoethyl conjugate appeared at 475–480 nm.

Extinction coefficients of the longest wavelength transition were estimated in the following way. A sample of acetylcholinesterase was completely inhibited with NBD-AE-MPF or NBD-AP-MPF. After gel filtration and dialysis, the protein conjugates lacked enzyme activity. The absorption spectrum of each conjugate at 280 nm served as a measure of enzyme concentration which was used to estimate the chromophore normality. For the NBD-aminoethyl methylphosphono-AchE conjugate, the extinction coefficient at the 475–480 nm transition was estimated to be 1.4 ± 0.2 × 10^4 M^{-1} cm^{-1}. The extinction coefficient for NBD-aminopentyl methylphosphono-AchE at the 485–490 nm transition was estimated to be 2.2 ± 0.2 × 10^4 M^{-1} cm^{-1}.

Reactivation of the NBD-aminoalkyl methylphosphonyl conjugates to 100% activity occurred in the presence of the bisquaternary oxime HI-6. Passage of the mixture through a Sephadex G-100 column to remove unbound NBD-aminoal-
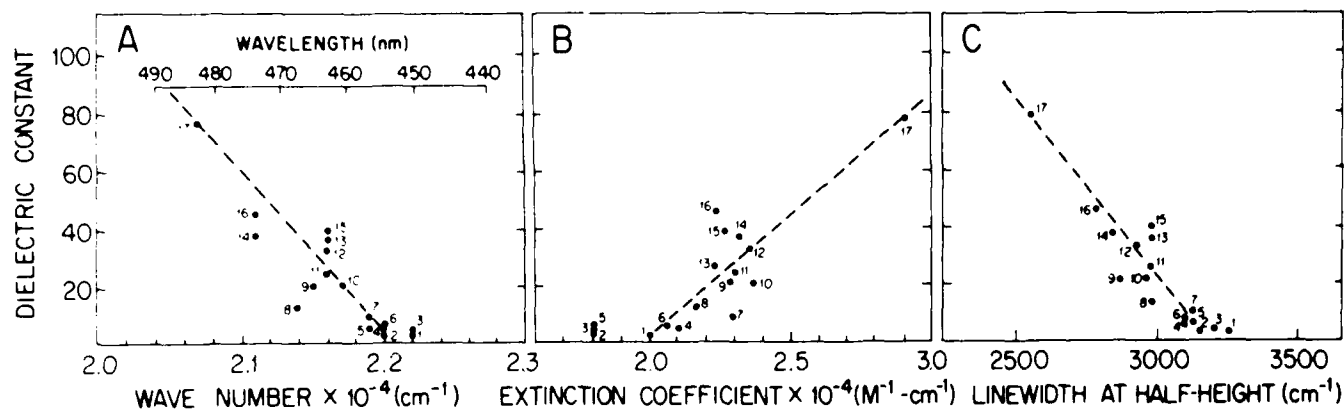
FIG. 2. **Relationship between absorption maximum, extinction coefficient, and spectral line width at half-height, and solvent dielectric constant for solutions of NBD-aminopentanol in a variety of organic solvents.** The absorption maxima and extinction coefficients at the longest wavelength were determined in a variety of organic solvents. *A*, the *abscissa* is represented as wave number (cm^{-1}); *B*, extinction coefficient at the absorption maximum (M^{-1} cm^{-1}); *C*, line width at half-height (cm^{-1}) for the 1 ← 0 transition. Dielectric constants were taken from Weast (36). The numbers denote the following solvents in order of increasing dielectric constant: *1*, dioxane; *2*, benzene; *3*, toluene; *4*, chloroform; *5*, bromobenzene; *6*, ethyl acetate; *7*, methylene chloride; *8*, pyridine; *9*, *n*-propanol; *10*, acetone; *11*, ethanol; *12*, methanol; *13*, nitromethane; *14*, dimethylformamide; *15*, acetonitrile; *16*, dimethyl sulfoxide; *17*, water.
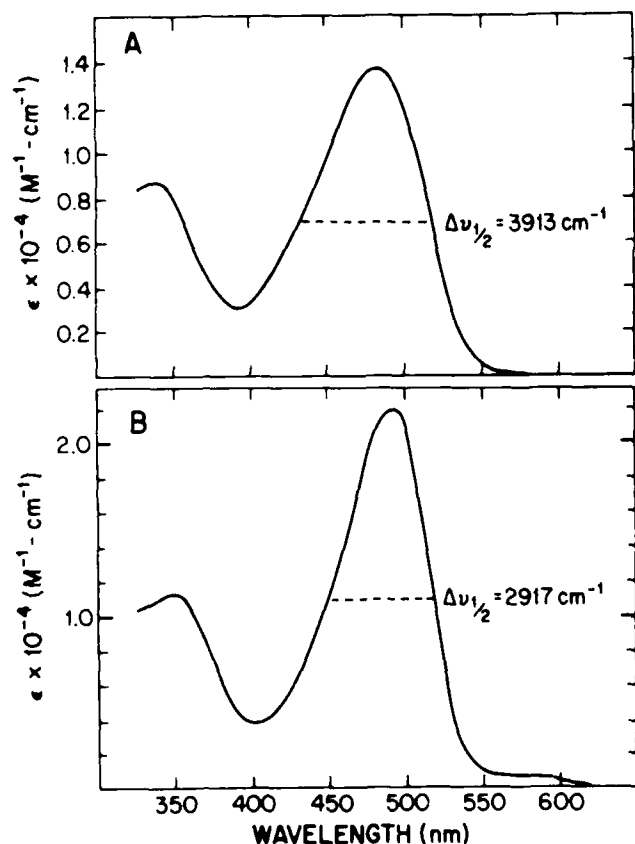

FIG. 3. **Absorption spectra of conjugates of NBD-amino-ethyl and NBD-aminopentyl methylphosphono-acetylcholinesterase.** *The data are presented as extinction coefficient* (M^{-1} cm^{-1}) *of NBD-aminoethyl methylphosphono-AchE (A) and NBD-amino-pentyl methylphosphono-AchE (B) present in a 0.01 N Tris-Cl buffer, pH 8.0, containing 0.1 N NaCl and 0.04 M MgCl$_2$.*

kanol and oxime resulted in complete loss of the chromophore. Thus, nonspecific labeling did not appear to occur.

Denaturation in 6 M urea shifted the absorption spectra of the NBD-aminoalkyl methylphosphonyl conjugates to wavelengths observed for the free probes in urea. The denatured

NBD-aminoethyl conjugate, however, exhibited a higher extinction coefficient than the nondenatured adduct. These data are reported in Table II along with results obtained with the 5.6 S dimeric form of acetylcholinesterase and α-chymotrypsin.

The (uncorrected) fluorescence spectra of the NBD-aminoethyl and NBD-aminopentyl methylphosphono-AchE conjugates, obtained upon excitation at the respective maxima, appeared at 525 and 530 nm, respectively. The fluorescence of the NBD-aminoalkyl moiety was highly quenched in aqueous environments while in less polar solvents, such as ethanol, the fluorescence quantum yield was appreciable. NBD-aminoethyl methylphosphono-AchE exhibited a fluorescence quantum yield that did not exceed 5% efficiency, as based on the value of fluorescein in 0.1 N NaOH (21), and was comparable to that obtained for the free probe in H$_2$O. The quantum yield for NBD-aminopentyl methylphosphono-AchE was consistently lower. Although absolute values of the fluorescence quantum yields were low, the relative differences observed were measurable and appear to reflect differences in the microscopic environments experienced by the respective homologs within the active center cleft.

The spectral linewidths at half-height ($\Delta\nu_{1/2}$) for both NBD-aminopentanol and NBD-aminoethanol in H$_2$O and 6 N urea were essentially equivalent and fall in the range 2600–2800 cm^{-1} (Table II). For the spectrum of NBD-aminopentyl methylphosphono-AchE, the linewidth at half-height was approximately 2.87 ± 0.05 × 10^3 cm^{-1}, a value comparable to that for the free probe in buffer, and underwent essentially no change upon denaturation of the conjugate in 6 M urea.

For the spectrum of NBD-aminoethyl methylphosphono-AchE, in contrast, the linewidth was approximately 3.87 ± 0.08 × 10^3 cm^{-1}, a value that was substantially greater than that observed for the NBD-aminopentyl adduct, and far greater than that observed in organic solvents (*cf.* Fig. 2C). Upon denaturation of the conjugate in 6 N urea, the width of this spectral band was decreased to a value (3.02 ± 0.05 × 10^3 cm^{-1}) similar to that observed for the free probe in buffer. The spectral band shapes for the enzyme conjugate could not be mimicked by immersion of NBD-aminoalkanol in any of the solvents examined.

Chiral Properties of NBD-aminoalkyl Methylphosphonyl Conjugates with Acetylcholinesterase—Chiral relationships at

TABLE II

Spectroscopic properties of NBD-aminoalkyl methylphosphonyl conjugates with acetylcholinesterase molecular forms

Values reported are the average ± S.D. over at least three determinations. Enzyme conjugates were present in a 0.01 N Tris-Cl buffer, pH 8.0, containing 0.1 N NaCl and 0.04 M MgCl$_2$. The dimeric 5.6 S molecular form was examined in the above buffer containing 0.1% Triton X-100.

	NBD-aminoethyl			NBD-aminopentyl		
	λ	$\epsilon \times 10^{-4}$	$\Delta\nu^{1/2} \times 10^{-3}$	λ	$\epsilon \times 10^{-4}$	$\Delta\nu^{1/2} \times 10^{-3}$
	nm	$M^{-1} cm^{-1}$	cm^{-1}	nm	$M^{-1} cm^{-1}$	cm^{-1}
H$_2$O[a]	475	2.5 ± 0.1	2.75 ± 0.06	480–485	2.8 ± 0.1	2.60 ± 0.14
6 N urea[a]	475	2.3 ± 0.1	2.75 ± 0.06	480–485	2.8 ± 0.1	2.57 ± 0.06
Acetylcholinesterase (11 S)	475–480	1.4 ± 0.2	3.87 ± 0.08	485–490	2.2 ± 0.2	2.87 ± 0.05
6 N urea	475	1.74 ± 0.02	3.02 ± 0.045	480–485	2.05 ± 0.03	2.83 ± 0.07
Acetylcholinesterase (5.6 S)	475		4.4 ± 0.4	490		3.1 ± 0.1
6 N urea						
α-Chymotrypsin	455–460	1.3 ± 0.1	3.36 ± 0.17	485–490	2.26 ± 0.02	2.72 ± 0.13
6 N urea	465	1.6 ± 0.2	3.25 ± 0.07	485	2.04 ± 0.09	2.63 ± 0.08

[a] When examined in H$_2$O and in 6 N urea, the probes were present as the NBD-aminoalkanols.

the active center of acetylcholinesterase were assessed by examining the circular dichroism of the NBD-aminoethyl and NBD-aminopentyl methylphosphono-AchE conjugates. Methylphosphonofluoridates, by virtue of an asymmetric phosphorus atom, would be predicted to exhibit optical activity. Such *intrinsic* optical activity is readily distinguished from *extrinsic* optical activity arising from association of the chromophore with a dissymmetric protein surface, since the latter but not the former phenomenon is abolished upon denaturation of the protein conjugate in 6 M urea.

The circular dichroism spectrum of NBD-aminopentyl methylphosphono-acetylcholinesterase (Fig. 4) exhibited intense optical activity characterized by a band shape and wavelength maximum consonant with the absorption spectrum. Optical activity at the absorption maximum was approximately 4500 degrees-cm^2/dmol. NBD-aminoethyl methylphosphono-AchE exhibited optical activity with maxima at 350 and 480 nm, consistent with the absorption spectrum, and an additional peak at 430 nm ($[\theta]_\lambda = 4100$ degrees-cm^2/dmol), a band not readily apparent in the absorption spectrum. The optical activity of both NBD-aminoethyl and NBD-aminopentyl methylphosphono-AchE was abolished upon denaturation of the conjugates in 6 M urea.

Spectral Characteristics of Conjugates with α-Chymotrypsin—Absorption spectra obtained for conjugates of the fluorescent methylphosphonates with α-chymotrypsin showed greater divergence between the NBD-aminoethyl and NBD-aminopentyl conjugates than observed for acetylcholinesterase. The spectrum of the NBD-aminopentyl methylphosphono-α-chymotrypsin adduct appeared at 480–485 nm ($\epsilon = 2.26 \pm 0.02 \times 10^4$ M^{-1} cm^{-1}) while the shorter chain NBD-aminoethyl adduct appeared at 455–460 nm ($\epsilon = 1.3 \pm 0.1 \times 10^4$ M^{-1} cm^{-1}), suggesting that the two congeners experience significantly different environments when covalently complexed with α-chymotrypsin. The bandwidths of the absorption spectra of NBD-aminopentyl and NBD-aminoethyl methylphosphonyl adducts with α-chymotrypsin were considerably narrower, $2.72 \pm 0.13 \times 10^3$ and $3.36 \pm 0.17 \times 10^3$ cm^{-1}, respectively, than those of the acetylcholinesterase conjugates. Denaturation of the chymotrypsin conjugates in 6 M urea exerted negligible effect on the spectral line widths.

The absorption transitions for NBD-aminoethyl methylphosphono-α-chymotrypsin between 300 and 550 nm were optically active; the maximum at 455 nm appeared with an intensity of approximately 2600 degrees-cm^2/dmol that was readily abolished upon denaturation in 6 M urea. The NBD-aminopentyl methylphosphono-α-chymotrypsin exhibited no detectable optical activity.
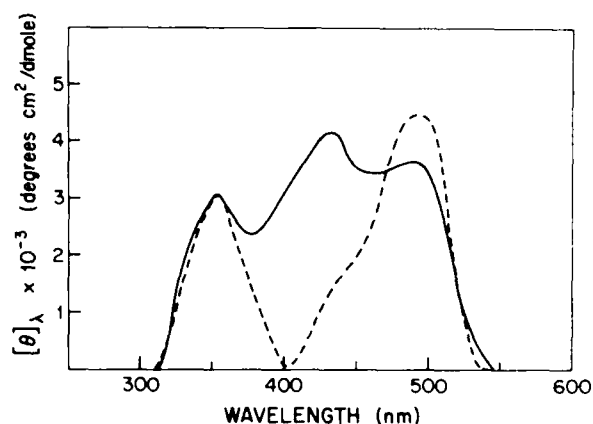

FIG. 4. **Circular dichroism spectra of conjugates of NBD-aminoethyl- and NBD-aminopentyl methylphosphono-acetylcholinesterase.** The figure presents molecular ellipticity (degrees-cm^2/decimole) *versus* wavelength (nanometers) for NBD-aminoethyl (——) and NBD-aminopentyl (- - - -) methylphosphono-acetylcholinesterase. Molecular ellipticity was calculated from Equation 1 where M_r of the chromophore was chosen as 207.17.
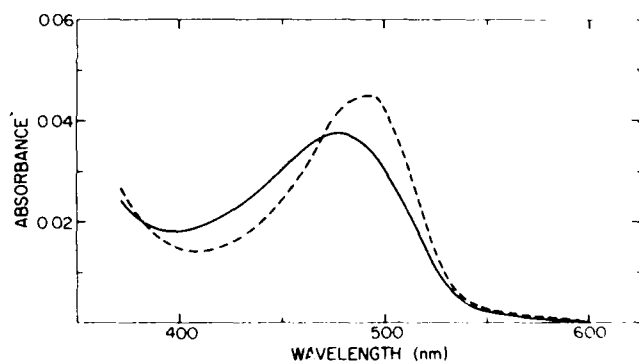

FIG. 5 **Absorption spectra of NBD-aminoethyl- and NBD-aminopentyl methylphosphonylconjugates of the dimeric molecular form of (5.6 S) acetylcholinesterase.** The enzyme was labeled with a 2-3-fold excess of agent, separated from unreacted material on a Sephadex G-25 gel filtration column, and dialyzed against a Tris-Cl buffer, pH 8.0, containing 0.1 N NaCl, 0.04 M MgCl$_2$, and 0.1% Triton X-100. The conjugate of NBD-aminoethyl (——) and NBD-aminopentyl (- - - -) methylphosphonofluoridates are shown.

Spectral Characteristics of Conjugates with the 5.6 S Dimeric Molecular Form of Acetylcholinesterase—Absorption spectra of conjugates of NBD-AE-MPF and NBD-AP-MPF with the

5.6 S hydrophobic dimeric molecular form of acetylcholinesterase from *Torpedo* showed absorption maxima that were essentially identical with those of the corresponding conjugates with the 11 S molecular form (Fig. 5 and Table II). The NBD-aminopentyl methylphosphonyl conjugate with the 5.6 S dimeric form of acetylcholinesterase exhibited an absorption maximum at 490 nm that was characterized by a spectral line width of 3.1 ± 0.1 × 10³ cm⁻¹, whereas the absorption maximum of the NBD-aminoethyl adduct at 475 nm was characterized by a line width at half-height of 4.4 ± 0.4 × 10³ cm⁻¹.

DISCUSSION

Association of NBD-aminoalkyl Methylphosphonofluoridates with Acetylcholinesterase—NBD-AE-MPF and NBD-AP-MPF are potent inhibitors of acetylcholinesterase hydrolytic activity, exhibiting inhibition rate constants exceeding 10⁵ M⁻¹ min⁻¹. By virtue of several independent criteria of intensity, position, and spectral bandwidth of the absorption and circular dichroism spectra and reactivation kinetics in the presence and absence of the bisquaternary oxime TMB-4, these agents form conjugates with acetylcholinesterase in which the chromophoric moiety experiences different microscopic regions within the active center. Modification of a common serine and the 2- and 5-carbon spacer groups separating the chromophore from the reactive methylphosphonyl group allows the NBD moiety to extend to different regions within the active center. Since they anchor on a single amino acid residue within the active center, the NBD-aminoalkyl probes can report on the protein environment within a perimeter conferred by the extended dimensions of the aminoalkyl chain, *i.e.* 7–12 Å.

The pre-existing tetrahedral symmetry of the phosphorus coordination sphere mimics the symmetry characteristic of the transition state during acetylcholine hydrolysis (4, 23, 24) and facilitates inhibition by organophosphonates. In addition, the dimensional compatibility of the methyl group and the dative P → O bond with the acyl pocket and oxyanion hole (23) further facilitates association of these agents, with the net result that the phosphonyl ester is directed in the exo-orientation toward the choline binding anionic subsite. In this study, the NBD-aminoalkyl moiety is expected to be in apposition with the anionic binding region of the active center and represents an orientation consistent with previous studies on pyrenebutyl methylphosphono-acetylcholinesterase (5, 6).

NBD-aminoethyl methylphosphonofluoridate appears susceptible to spontaneous hydrolysis while the NBD-aminopentyl isomer is resistant to such degradation. Electron delocalization by the nitro group endows the NBD moiety with a substantial dipole moment in which the amino group carrying a partial positive charge is stabilized through interaction with the electronegative P → O bond within the 6-membered cyclic intermediate (3). Such intramolecular stabilization enhances electrophilicity of the

F 3

F 4
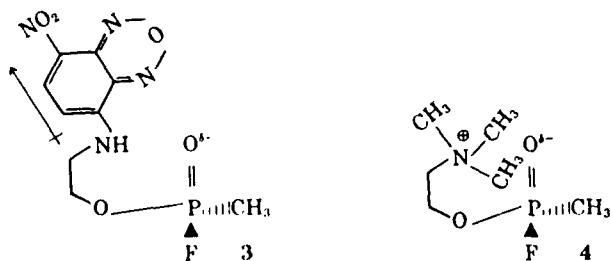
tetrahedral phosphonyl atom and makes it more susceptible to attack by H₂O. The 5-carbon homolog, NBD-aminopentyl methylphosphonofluoridate, cannot adopt this conformation. Support for such a mechanism is derived from observations

that β-(trimethylammonium)ethyl methylphosphonofluoridate, a potent cationic inhibitor of acetylcholinesterase (25, 26), is readily hydrolyzed in buffer at pH 8.0 with a rate constant of 0.47 ± 0.05 min⁻¹ ($t_{1/2}$ = 1.5 min).² Rapid hydrolysis appears to represent a general property of a subgroup of those methylphosphonofluoridates which exhibit the capacity to form intramolecularly stabilized conformations.

Reactivation of NBD-aminoalkyl Methylphosphono-acetylcholinesterase—Reactivation of organophosphonyl-AchE conjugates occurs by displacement of the organophosphonyl moiety from the enzyme active center surface following either complexation of cationic oximes at the anionic subsite (22) or direct reaction with H₂O. Since both spontaneous and oxime-induced reactivation are dependent on organophosphonate structure (*cf.* Table I), the reactivation rates in the presence of oxime cannot be attributed solely to diminished complexation of the oxime with the modified enzyme. Hence, the difference in rates likely reflects a difference in access of the attacking nucleophile to the phosphonylated serine. These rate differences reflect in part the capacity of the 5-carbon chain to interact more tightly with the active center cleft (27), thereby precluding reaction with H₂O, as well as the strength of dipolar interaction of the NBD entity with the anionic surface of the enzyme. Such an explanation predicts nonequivalence of the NBD aminoalkyl sites of contact within the active center, and the spectral characteristics to be discussed below provide a direct assessment of this nonequivalence.

Spectroscopic Characterization of the NBD-aminoalkyl Methylphosphono-AchE Conjugates—Upon transfer of NBD-aminopentanol from solvents of high to low polarity, as measured by solvent dielectric constant, the absorption and fluorescence maxima are shifted to shorter wavelength, the extinction coefficient is diminished, and in general, the fluorescence quantum efficiency is increased. These observations are consonant with those obtained for NBD-5-acylcholine (31–33) and 4-bis-(choline)N-[4-nitrobenz-2-oxa-1,3-diazol-7-yl] iminodipropionate (34), analogs of acetylcholine which associate reversibly at the active center of acetylcholinesterase, and NBD-alanine (20). As seen in Fig. 2, however, the correlations are not perfect and, compared with the data of Table II, the spectral characteristics of the protein conjugates do not follow those of the free probes immersed in organic media in several important respects.

The absorption spectrum of NBD-aminoethyl methylphosphono-AchE approaches a maximum value of 480 nm, similar to the value found for the chromophore in H₂O, whereas the extinction coefficient of the enzyme adduct approximates the value seen in aromatic solvents. Absorption maxima for NBD-aminopentyl methylphosphono-AchE appear approximately 5 nm to the red of that seen in H₂O. This behavior could not be reproduced in any of the organic solvents studied. These results for acetylcholinesterase contrast with those for conjugates with α-chymotrypsin which show a clear correspondence between wavelength maxima, extinction coefficient, and solvent dielectric constant. NBD-aminoethyl methylphosphono-AchE has an absorption spectrum that is approximately 1000 cm⁻¹ broader at half-maximum than that of the corresponding NBD-aminopentyl conjugate and is substantially broader than the spectrum of the free probe in organic media (*cf.* Fig. 2C). Finally, NBD-aminoethyl methylphosphono AchE shows strong optical activity (Fig. 4) at wavelengths corresponding to the regions of spectral broadening, suggesting a common origin for both phenomena. No such spectral broadening or pattern of optical activity are observed for NBD-aminopentyl methylphosphono-acetylcholinester-

² H. A. Berman, unpublished observations.

ase and NBD-aminoethyl methylphosphono-α-chymotrypsin. Since the spectral characteristics and line broadening of the protein conjugates are altered or abolished upon denaturation in urea, the position, band shape, and optical activity of NBD-aminoalkyl conjugates with acetylcholinesterase are attributable to molecular characteristics of the binding site, and the 2- and 5-carbon congeners are concluded to be in contact with different microscopic environments within the active center cleft.

The most likely explanation for the spectral broadening proposes the presence of a charge-transfer complex between the NBD-aminoethyl chromophore and an aromatic amino acid within the binding site. Charge-transfer complexation requires direct overlap of the molecular orbitals of donor and acceptor molecules within their molecular diameters (28) and would require the NBD-aminoethyl moiety to associate in a region containing an aromatic residue.

One plausible candidate as a charge-transfer donor would be a tryptophanyl residue within the active center. This proposal gains support from observations that NBD-alanine readily exhibits charge-transfer spectra in the presence of aromatic molecules (20). More specifically, association of N-methylacridinium at the active center of eel acetylcholinesterase results in pronounced formation of a charge-transfer complex that has been attributed to the presence of a tryptophanyl residue within 5 Å of the active center surface (29).

The appearance of charge-transfer interactions for the NBD-aminoethyl but not the NBD-aminopentyl methylphosphonyl conjugate of acetylcholinesterase and neither of the conjugates with α-chymotrypsin signifies the presence of a tryptophanyl residue within 4 bond lengths (approximately 7 Å) of the methylphosphono-serine linkage in acetylcholinesterase. Interposition of an additional 3 bond lengths (5 Å) is adequate to abolish such molecular overlap and, in turn, the capacity for donor-acceptor interactions.

Comparison of Different Molecular Forms of Acetylcholinesterase—Comparison of the absorption spectra of the NBD-aminoalkyl methylphosphono-AchE adducts (*cf.* Table II) reveals the active center protein environment of the 11 S lytic and the 5,6 S hydrophobic dimeric molecular forms to be equivalent. This result is interesting in view of evidence that these molecular forms of acetylcholinesterase, although derived from the same *Torpedo* species, show differences in their tryptic peptides, antigenic components, and primary sequences and appear to be the product of different genes (35). Although sequence comparison reveals substantial regions where homology is not found, both molecular forms show [³H] diisopropylphosphorofluoridate-containing peptides that are very similar if not identical. The virtually identical absorption spectra obtained with dimensionally distinct spectroscopic probes afford an assessment independent of sequence analysis that the active center of these two genetically distinct forms of acetylcholinesterase are dimensionally and chemically equivalent.

Although the overall primary sequences of the serine proteases and acetylcholinesterase appear unrelated, the amino acid sequence in the region of the reactive serine residue for acetylcholinesterase from electrophorus and α-chymotrypsin

appear to show homology and are strongly conserved (30), as are the corresponding catalytic mechanisms (4, 23). Comparison of the NBD-aminoalkyl methylphosphonyl conjugate formed with α-chymotrypsin and acetylcholinesterase from *Torpedo* indicates that the active center protein environments are not identical. Lack of any discernible optical activity, since it arises from *extrinsic* mechanisms, indicates that the NBD-aminopentyl moiety experiences negligible contact with the α-chymotrypsin surface, a situation in contrast with that for acetylcholinesterase but consistent with the peptide substrate specificity and greater torsional mobility about the active serine residue within the dimensionally less restrictive protease active center (37).

REFERENCES

1. Berman, H. A., Yguerabide, Y., and Taylor, P. (1980) *Biochemistry* 17, 2226-2235
2. Taylor, P., and Lappi, S. (1975) *Biochemistry* 14, 1989-1997
3. Mooser, G., and Sigman, D. S. (1974) *Biochemistry* 13, 2299-2307
4. Rosenberry, T. L. (1975) *Adv. Enzymol. Relat. Areas Mol. Biol.* 43, 103-218
5. Berman, H. A., and Taylor, P. (1978) *Biochemistry* 17, 1704-1713
6. Berman, H. A., Becktel, W., and Taylor, P. (1981) *Biochemistry* 20, 4803-4810
7. Amitai, G., Ashani, Y., Gafni, A., and Silman, I. (1982) *Biochemistry* 21, 2060-2069
8. Kenner, R. A., and Aboderin, A. A. (1971) *Biochemistry* 10, 4433-4440
9. Taylor, P., and Jacobs, N. M. (1974) *Mol. Pharmacol.* 10, 93-107
10. Viratelle, O. M., and Bernhard, S. A. (1980) *Biochemistry* 19, 4999-5007
11. Lee, S. L., Camp, S. J., and Taylor, P. (1982) *J. Biol. Chem* 257, 12302-12309
12. Adler, A. J., Greenfield, N. J., and Fasman, G. D. (1973) *Methods Enzymol.* 270, 675-735
13. Hart, G. J., and O'Brien, R. D. (1973) *Biochemistry* 12, 2940-2945
14. Hart, G. J., and O'Brien, R. D. (1974) *Pestic. Biochem. Physiol.* 4, 239-244
15. Voss, H. F., Ashani, Y., and Wilson, I. B. (1975) *Methods Enzymol.* 34, 581-591
16. Tullock, C. W., and Coffman, D. D. (1960) *J. Org. Chem* 25, 2016-2019
17. Dawson, T. P., and Kennard, K. C. (1957) *J. Org. Chem.* 22, 1671-1672
18. Main, A. R., and Iverson, F. (1966) *Biochem. J.* 100, 525-531; Main, A. R. (1964) *Science (Wash. D. C.)* 144, 992-993.
19. Ashani, Y., Wins, P., and Wilson, I. B. (1972) *Biochim. Biophys. Acta* 284, 427-434
20. Lancet, D., and Pecht, I. (1977) *Biochemistry* 16, 5150-5157
21. Parker, C. A., and Rees, W. T. (1960) *Analyst* 85, 587-600
22. Aldridge, W. N., and Reiner, E. (1972) *Enzyme Inhibitors as Substrates*, North-Holland, Amsterdam
23. Kraut, J. (1977) *Annu. Rev. Biochem.* 46, 331-358
24. Wolfenden, R. (1972) *Accts. Chem. Res.* 5, 10-18
25. Tammelin, L.-E. (1957) *Acta Chem. Scand.* 11, 1340-1349
26. Larsson, L. (1957) *Acta Chem. Scand.* 11, 1131-1142
27. Kabachnik, M. I., Brestkin, A. P., Godovikov, N. N., Michelson, M. J., Rozengart, F. V., and Rozengart, V. I. (1970) *Pharmacol. Rev* 22, 355-388
28. Foster, R. (1969) *Organic Charge-Transfer Complexes*, Academic Press, London
29. Shinitzky, M., Dudai, Y., and Silman, I. (1973) *FEBS Letters* 30, 125-128
30. Schaffer, N. K., Michel, H. O., and Bridges, A. F. (1973) *Biochemistry* 12, 2946-2950
31. Jurss, R., Prinz, H., and Maelicke, A. (1979) *Proc. Natl. Acad. Sci. U. S. A* 76, 1064-1068
32. Prinz, H., and Maelicke, A. (1983) *J. Biol. Chem* 258, 10263-10271
33. Jurss, R., and Maelicke, A. (1981) *J. Biol. Chem* 256, 2887-2893
34. Bolger, M. B., Dionne, V., Chrivia, J., Johnson, D. A., and Taylor, P. (1984) *Mol. Pharmacol.* 26, 57-69
35. Doctor, B. P., Camp, S., Gentry, M. K., Taylor, P. (1983) *Proc. Natl. Acad. Sci. U. S. A* 80, 5767-5771
36. Weast, R. C., Ed. (1981) in *CRC Handbook of Chemistry and Physics*, 62nd ed., pp. E52-54, CRC Press, Inc., Boca Raton, FL
37. Sentjurc, M., Stalc, A., and Zupancic, A. O. (1976) *Biochim. Biophys. Acta* 438, 131-137 (and references therein)